Available online at www.sciencedirect.com

ScienceDirect

International Journal of Solids and Structures 45 (2008) 1352–1384

INTERNATIONAL JOURNAL OF SOLIDS AND STRUCTURES

www.elsevier.com/locate/ijsolstr

Elastic and piezoelectric fields due to polyhedral inclusions

Boris N. Kuvshinov *

Shell International Exploration and Production B.V., Kessler Park 1, 2288 GS Rijswijk, The Netherlands

Received 16 April 2007; received in revised form 25 September 2007
Available online 1 October 2007

Abstract

We derive explicit, closed-form expressions describing elastic and piezoelectric deformations due to polyhedral inclusions in uniform half-space and bi-materials. Our analysis is based on the linear elasticity theory and Green's function method. The method involves evaluation of volume and surface integrals of harmonic and bi-harmonic potentials. In case of polyhedra, such integrals are expressed through algebraic functions. Our results generalize numerous studies on this subject, and they allow to obtain fully analytical solutions for a number of physical and engineering problems. In the limiting case of an infinite space, our relations have an essentially more compact form, than relations obtained by other authors. We present solutions to classical Mindlin and Cherruti problems. We describe the elastic relaxation of a misfitting polygonal quantum dot in bi-materials assuming isotropic and vertically isotropic properties. It is explained how to analyze non-hydrostatic and non-uniform inclusions. We also study piezoelectric fields induced by inclusions in materials with cubic and hexagonal lattices. Among other results, we have found that a cubic inclusion in an isotropic material reproduces fields of quantum dots in GaAs $(0,0,1)$ and GaAs $(1,1,1)$ depending on the orientation of the cube. This suggests that one can qualitatively model crystals with different lattices by choosing an appropriate inclusion shape.

Keywords: Polyhedral quantum dots; Linear elasticity; Green's functions; Anisotropy; Piezoelectric field

1. Introduction

Analysis of mechanical deformations induced by misfitting inclusions in an infinite or semi-infinite elastic medium is a fundamental physical and engineering problem, which has roots in 19th century (Thomson, 1882; Cerutti, 1882; Boussinesq, 1885). It has been originally studied within the context of thermoelasticity and mechanics of solids (Mindlin, 1936; Goodier, 1937; Mindlin and Cheng, 1950; Sen, 1951; Eshelby, 1957) and then in seismology and geophysics (Geertsma, 1957; Steketee, 1958; Rongved and Frazier, 1958; Geertsma, 1973). Reviews of earlier research on this subject can be found in books by Nowacki (1986) and Mura (1987).

The rapid development of nanotechnology in last years has brought a renewed interest to the above classical problem. A number of modern semiconductor devices, such as lasers, infrared detectors, and information storage devices use composite materials, where tiny objects with the size of several nanometers are buried in

* Tel.: +31 70 447 2932.
E-mail address: Boris.Kuvshinov@Shell.com

0020-7683/$ - see front matter
doi:10.1016/j.ijsolstr.2007.09.024

the surrounding matrix (Rinaldi et al., 1994; Bimberg et al., 1998; Harrison, 1999; Cui and Lieber, 2001). These objects are commonly called quantum dots, or quantum wires if they are extended in one of the dimensions. Quantum dots induce elastic and piezoelectric deformations, which strongly influence properties of the composite materials and hence the performance of devices. Calculations of corresponding deformations have attracted significant attention in the literature (Grundmann et al., 1995; Shchukin et al., 1998; Davies, 1998; Faux and Pearson, 2000). Recent reviews by Stangl and Holý (2004); Maranganti and Sharma (2005); Ovid'ko and Sheinerman (2005, 2006) provide a detail discussion of these studies.

Elastic deformations due to quantum dots are found using an atomistic approach (Cusack et al., 1997; Makeev and Madhukar, 2001; Kikuchi et al., 2001; Kohler, 2003; Wang and Li, 2004) or from continuum elasticity (Grundmann et al., 1995; Pryor et al., 1997). As has been shown by Pryor et al. (1998), both methods agree for small deformations. Equations of continuum elasticity can be solved numerically, using a finite difference method (Grundmann et al., 1995), a finite element method (Benabbas et al., 1996; Johnson and Freund, 2001), a boundary element method (Yang and Pan, 2002), or an energy minimization method (Jogai, 2000). Although numerical simulations provide a complete solution to the problem, analytical calculations still play an important role. In a number of studies it has been confirmed that descriptions of quantum dots using idealized analytical models and more rigorous numerical techniques are in good agreement (Daruka et al., 1999; Andreev et al., 1999; Romanov et al., 2001, 2005; Jonsdottir et al., 2006). Exact analytical formulas can significantly facilitate analysis of material properties. They also provide a benchmark for codes, and are helpful to obtain a better physical insight.

Analytical results can be roughly split in two groups. First, these are semi-analytical equations, which require additional numerical calculations to get the desired answer. Examples are solutions in Fourier space (Downes and Faux, 1997; Andreev et al., 1999; Andreev and O'Reilly, 2000) and solutions written in terms of series expansion (Ru et al., 2001; Faux and Christmas, 2005). Second, these are fully analytical formulas, where the answer is expressed through elementary or special functions. Such formulas are available for three-dimensional inclusions in an infinite space or in half-space, which have the shape of an ellipsoid (Eshelby, 1957; Seo and Mura, 1979), and disk (Wu and Du, 1995a,b, 1996; Glas, 2003).

Majority of analytical solutions are obtained by using the Green tensor approach. One finds elastic deformations due to a point-wise inclusion (Mindlin and Cheng, 1950; Sen, 1951), and then integrate the result over the volume of the actual inclusion. Recent examples of such an approach are given by Pan (2002c); Yang and Pan (2003); Pan (2004a); Chu and Wang (2005). Calculations can be simplified by reducing volume integrals to integrals over the inclusion surface (Yu et al., 1994; Downes et al., 1997). Since the elastic deformations are described by harmonic and bi-harmonic potentials (Eshelby, 1957), the integration procedure is essentially the same as in the theory of Newtonian potential (MacMillan, 1930). MacMillan (1930) explains how to integrate the gravitational potential over cuboidal bodies. Waldvogel (1979) has developed an algorithm, based on a three dimensional triangulation of the inclusion, to perform this integration over polyhedra. This algorithm has been used by Rodin (1996) and by Nozaki and Taya (1997) to analyze the Eshelby problem for polyhedral inclusion in an infinite space.

Rodin (1996) and Nozaki and Taya (1997) present explicit formulas for two-dimensional inclusions, which are infinitely extended in one dimension and have a constant cross-section. In nanotechnological applications such inclusions are called quantum wires. In this case one deals only with contour integrals over the wire boundary (Downes et al., 1995; Faux et al., 1996). This circumstance has helped to carry out a rather extensive analysis of quantum wires. Explicit expressions have been obtained for the trapezoidal (Gossling and Willis, 1995), as well as for rectangular, triangular, and circular quantum wires embedded in an infinite uniform space (Faux et al., 1997). Relatively simple explicit formulas for polygon inclusions have been derived by Kawashita and Nozaki (2001). Glas (2002a), Davies (2003), Gutkin et al. (2003) have studied hydrostatic rectangular and trapezoidal wires in an isotropic half-space. Wires with polygonal cross-sections in anisotropic full and half-spaces have been analyzed by Pan (2004a,b). Ru (1999, 2000, 2001, 2003) has developed a conformal mapping method, which provides an implicit solution of the problem for wires with arbitrary cross-sections. Polygonal inclusions have been also studied by Jiang and Pan (2004) and Pan et al. (2007) taking into account anisotropic and magnetoelectric effects.

There exists another class of two-dimensional inclusions, which in contrast to quantum wires have a negligibly small length in one of the dimensions. Such inclusions are studied in the dislocation theory (Steketee, 1958), which

is frequently applied to nanomaterials (Gutkin, 2006). Analytical solutions describing rectangular dislocations in a half-space have been derived by Chinnery (1961, 1963) and Okada (1985, 1992). Inclusions with a rectangular and circular cross-sections in an infinite plate have been analyzed by Beom and Kim (1999) and Tian and Rajapakse (2007) correspondingly. Comninou and Dundurs (1975) give expressions for displacements and strains at the free surface of a half-space due to angular dislocations. By combining angular dislocations one can model arbitrary polygon-shaped dislocations. The model of Comninou and Dundurs (1975) has been implemented in the Stanford Poly3D code (Thomas, 1993), which is used in geophysical applications (Maerten et al., 2005).

To investigate three-dimensional effects in quantum dots one can consider them as spherical inclusions (Sharma and Dasgupta, 2002; Sharma and Ganti, 2004; Duan et al., 2005; Mi and Kouris, 2006). Most commonly, quantum dots have a polyhedron shape. The first particular case of a polyhedral inclusion, which has been studied analytically, was a cuboidal (parallelepipedic) inclusion. Ignaczak and Nowacki (1958) (see book by Nowacki (1986)) have derived expressions for the stress field outside a cuboidal inclusion in an infinite uniform space. They have analyzed a thermoelastic problem, where the eigenstrain in the inclusion is hydrostatic. These results have been generalized for cuboidal inclusions with a dilatation strain by Faivre (1964) by Chiu (1977). An alternative derivation is given by Li and Anderson (2001). Nozaki and Taya (2001) have used the algorithm of Waldvogel, 1979 to describe polyhedral inclusions in an infinite space. They have presented an analytical solution to the problem, although in a complicated form. Chiu (1978) has considered hydrostatic cuboidal inclusions in a half-space. He has got an implicit solution in terms of Legendre functions for strains parallel to the half-space boundary and for stresses. Hu (1989) has derived explicit expressions for stresses outside of a cuboidal inclusion. Glas (1991) has extended the work of Hu (1989) by calculating displacements and the energy of deformations. The elastic field induced by a truncated pyramidal inclusion with a hydrostatic eigenstrain has been calculated by Pearson and Faux (2000) and Stoleru et al. (2002) for the case of an infinite isotropic medium, and by Glas (2001, 2002b) for the case of a half-space. Apparently, solutions of Glas (2001, 2002b) are the most general, three-dimensional analytical solution, which have been derived so far.

Available analytical solutions either represent too simplistic cases, or they are rather incomprehensive, which restrict their usefulness. A similar situation occured in geophysical prospecting in analysis of gravitational and magnetic anomalies (Strakhov and Lapina, 1990; Li and Chouteau, 1998; Holstein et al., 1999; Holstein, 2002). Original calculations of such fields produced by polyhedral bodies have been done in a Cartesian coordinate system (Paul, 1974; Okabe, 1979). This approach leads to equations, which are difficult to use in practice. Later it was recognized, that the above equations possess a number of invariant properties (Strakhov et al., 1986). Various geometrical parameters representing polyhedra enter the integrals as constant multiplicative factors. This allows to carry out the integration in a compact, coordinate-free form, and to express the answer in terms of few standard integrals (Pohánka, 1988; Götze and Lahmeyer, 1988; Holstein and Ketteridge, 1996).

Analysis of elastic deformations is more difficult than analysis of gravitational anomalies, because one needs to treat several different integrals rather than a single integral of the Newtonian potential. Nevertheless, calculations of correspondent integrals can be also carried out in a coordinate-free form. In this paper we perform such an integration for three-dimensional polyhedral inclusions in a half-space or uniform bi-materials, which are isotropic or transversely isotropic. In Section 2 we introduce starting equations. Complete solution to the problem in a uniform and isotropic infinite space is given in Section 3. In Section 4 we present equations describing hydrostatic inclusions in isotropic bi-materials. We also consider a particular case of cuboidal inclusions, which shows how results of previous studies can be reconstructed using our procedure. Section 5 explains how to generalize our procedure to describe non-uniform inclusions, non-hydrostatic inclusions, and to include effects of anisotropy. The general theoretical approach developed in first Sections is applied in Section 6 to analyze piezoelectric fields induced by quantum dots. Section 7 summarizes the results. Appendices A, B, C contain details of calculations.

2. Elastic equilibrium

We consider polyhedral inclusions in a half-space or in a bi-material medium. The spatial coordinates are denoted as x_j with $j = 1, 2, 3$. The plane $z \equiv x_3 = 0$ coincides with the interface. The z-axis is directed towards the inclusion. In what follows we calculate elastic deformations in the part of the space, occupied by the inclusion, i.e. at $z > 0$.

Static deformations of an elastic medium are described by the momentum balance equation

$$0 = \nabla \cdot \overleftrightarrow{\boldsymbol{\sigma}} + \vec{\boldsymbol{F}}, \tag{1}$$

where $\vec{\boldsymbol{u}}$ is the solid displacement, $\overleftrightarrow{\boldsymbol{\sigma}}$ is the stress tensor, and $\vec{\boldsymbol{F}}$ is the external force. Eq. (1) is supplemented by the stress–strain relation, which is commonly written in the form (Mura, 1987),

$$\sigma_{ij} = C_{ijmn}\left(e_{mn}^{(\mathrm{eff})} - e_{mn}^{(I)}\right) = C_{ijmn}e_{mn}. \tag{2}$$

Here, $e_{mn}^{(\mathrm{eff})}$ is the effective strain tensor, which is related to the solid displacement $\vec{\boldsymbol{u}}$ as

$$e_{mn}^{(\mathrm{eff})} = (u_{m,n} + u_{n,m})/2, \tag{3}$$

$e_{mn}^{(I)}$ is the misfitting strain tensor due to inclusion, C_{ijmn} is the tensor of elastic moduli, and a comma in the subscript denotes derivative with respect to spatial coordinates, e.g. $u_{m,n} \equiv \partial u_m/\partial x_n$.

The tensor C_{ijmn} in an isotropic medium simplifies to

$$C_{ijmn} = \lambda\delta_{ij}\delta_{mn} + \mu(\delta_{im}\delta_{jn} + \delta_{in}\delta_{jm}), \tag{4}$$

where λ and μ are Lamé constants and δ_{ij} is the Kronecker delta. Combining Eqs. (1)–(4) one casts the elastic equilibrium in the form of the Navier equation,

$$(H-\mu)\nabla\nabla\cdot\vec{\boldsymbol{u}} + \mu\nabla^2\vec{\boldsymbol{u}} = \nabla\cdot\overleftrightarrow{\boldsymbol{\sigma}}^{(I)} - \vec{\boldsymbol{F}}. \tag{5}$$

Here, $H = \lambda + 2\mu$ and $\overleftrightarrow{\boldsymbol{\sigma}}^{(I)}$ is the inclusion stress tensor, $\sigma_{ij}^{(I)} = C_{ijmn}e_{mn}^{(I)}$. The stress tensor of a hydrostatic inclusions with $e_{mn}^{(I)} = e^{(I)}\delta_{mn}$ is equal to, $\sigma_{ij}^{(I)} = p^{(I)}\delta_{ij}$, where

$$p^{(I)} = (3\lambda + 2\mu)e^{(I)} = 2\mu\frac{1+\nu}{1-2\nu}e^{(I)} = \frac{Ee^{(I)}}{1-2\nu}, \tag{6}$$

$\nu = \lambda/(2(\lambda+\mu))$ is the Poisson ratio, and $E = 2\mu(1+\nu)$ is the Young modulus. A hydrostatic inclusion with the eigenstrain $e^{(I)}\delta_{mn}$ induces the same deformation as the external force $\vec{\boldsymbol{F}} = -\nabla p^{(I)}$, where $p^{(I)}$ is given by Eq. (6).

The Green tensor $G_{ij}(\vec{\boldsymbol{r}}, \vec{\boldsymbol{r}}')$ for Navier Eq. (5) is determined by the condition

$$(H-\mu)G_{ij,is} + \mu G_{sj,ii} = -\delta_{js}\delta(\vec{\boldsymbol{r}} - \vec{\boldsymbol{r}}'). \tag{7}$$

Here, $\vec{\boldsymbol{r}}'$ is the position of a delta-functional inclusion, or the point where an external force is applied. The function $u_i(\vec{\boldsymbol{r}}) = G_{ij}(\vec{\boldsymbol{r}}, \vec{\boldsymbol{r}}')$ is the solution of Eq. (5), provided its right side is equal to $\nabla\cdot\overleftrightarrow{\boldsymbol{\sigma}}^{(I)} - \vec{\boldsymbol{F}} = -\delta(\vec{\boldsymbol{r}} - \vec{\boldsymbol{r}}')\vec{\boldsymbol{e}}_j$, where $\vec{\boldsymbol{e}}_j$ is the unit vector along the coordinate x_j. If the right side of Eq. (5) is equal to $-\delta_{,k'}(\vec{\boldsymbol{r}} - \vec{\boldsymbol{r}}')\vec{\boldsymbol{e}}_j$, then its solution is obtained by differentiating the above Green tensor, $u_i(\vec{\boldsymbol{r}}) = G_{ij,k'}(\vec{\boldsymbol{r}}, \vec{\boldsymbol{r}}')$. The subscript "$k'$" after comma indicates that the derivative is taken with respect to x_k'. The general solution of Eq. (5) in the absence of external forces, $\vec{\boldsymbol{F}} = 0$, is equal to (Mura, 1987)

$$u_i(\vec{\boldsymbol{r}}) = \int_V C_{jkmn}e_{mn}^{(I)}(\vec{\boldsymbol{r}}')G_{ij,k'}(\vec{\boldsymbol{r}}, \vec{\boldsymbol{r}}')\mathrm{d}\vec{\boldsymbol{r}}'. \tag{8}$$

The integration in Eq. (8) is carried out over the volume V occupied by the inclusion.

3. Infinite space

Uniform polyhedral inclusions in a uniform and isotropic infinite space is the simplest situation to be analyzed. In case of hydrostatic inclusions, we derive explicit expressions for the displacement. Arbitrary inclusions are described by the Eshelby tensor, which has a relatively simple form compared to the expression presented by Nozaki and Taya, 2001.

3.1. Hydrostatic inclusions

Since the curl of the solid displacement must vanish for hydrostatic inclusions, $\nabla \times \vec{\boldsymbol{u}} = 0$, Eq. (5) reduces to the Poisson equation whose solution is written as (Downes et al., 1997; Davies, 1998),

$$\vec{\boldsymbol{u}} = -\frac{p}{4\pi H}\nabla\Phi = -\frac{e}{4\pi}\frac{1+v}{1-v}\nabla\Phi. \tag{9}$$

Here, Φ is the Newtonian potential, $\Phi(\vec{\boldsymbol{r}}) = \int_V \mathrm{d}\vec{\boldsymbol{r}}'/R$, $R = |\vec{\boldsymbol{R}}|$, and $\vec{\boldsymbol{R}} = \vec{\boldsymbol{r}}' - \vec{\boldsymbol{r}}$. The integral of the gravitational potential over the polyhedral bodies has been derived by several authors (Pohánka, 1988; Holstein and Ketteridge, 1996). An alternative derivation is given in Appendix A, where we use a more general approach. Taking into account that $\nabla\int_V \mathrm{d}\vec{\boldsymbol{r}}'/R = -\int_V \nabla'(1/R)\mathrm{d}\vec{\boldsymbol{r}}'$, where ∇' is the gradient operator in the $\vec{\boldsymbol{r}}'$-space, one has

$$\Phi_{,i} = \sum_{\text{polygons}} n_i \sum_{\text{edges}} (R_b I_{-1} + R_n J_{-1} - |R_n|\theta), \tag{10}$$

and

$$\Phi_{,ij} = \sum_{\text{polygons}} n_i \sum_{\text{edges}} \left(b_j I_{-1} + n_j J_{-1} - n_j \frac{R_n}{|R_n|}\theta \right). \tag{11}$$

Here, the summation is carried over polygons constituting the polyhedron surface and over their edges, $\vec{\boldsymbol{n}}$, $\vec{\boldsymbol{b}}$, and $\vec{\boldsymbol{v}}$ are local coordinate vectors explained in Fig. 1, subscripts n, b, and v denote projections along these vectors, e.g. $R_n = \vec{\boldsymbol{R}}\cdot\vec{\boldsymbol{n}}$, subscripts i and j denote projections along Cartesian coordinate vectors, e.g. $n_i = \vec{\boldsymbol{n}}\cdot\vec{\boldsymbol{e}}_i$. The integrals I_q and J_q are determined by Eqs. (A.9) and (A.10), the apex angle θ is equal to $\theta = \arctan(R_v/R_b)|_{\tau_1}^{\tau_2}$, where τ_1 and τ_2 label the beginning and the end of each of the edges, and we use the standard notation $g|_x^y = g(y) - g(x)$ for any function g.

Eqs. (9)–(11), are sufficient to obtain explicit expressions for strains and stresses. The displacement and its derivatives are determined by the same set of algebraic functions I_{-1}, J_{-1}, and θ. This circumstance has been discussed by Holstein, 2002 within the context of the similarity between the gravitational and magnetic potentials of polyhedra.

3.2. Geometric interpretation

It is convenient to interpret Eq. (11) in terms of solid angles Ω (Holstein, 2002), which is similar to the interpretation of electrostatic potentials due to double layers (Stratton, 1941). The differential solid angle $\mathrm{d}\Omega$ is defined as $\mathrm{d}\Omega = -\nabla(1/R)\cdot\mathrm{d}\vec{\boldsymbol{S}}$ (Stratton, 1941). According to this definition the sign of Ω coincides with the sign of R_n. Eq. (11) can be written in the form

$$\Phi_{,ij} = \sum_{\text{polygons}} n_i \sum_{\text{edges}} (b_j I_{-1} - n_j \Omega). \tag{12}$$

which is useful to estimate influence of the inclusion shape on induced stresses.

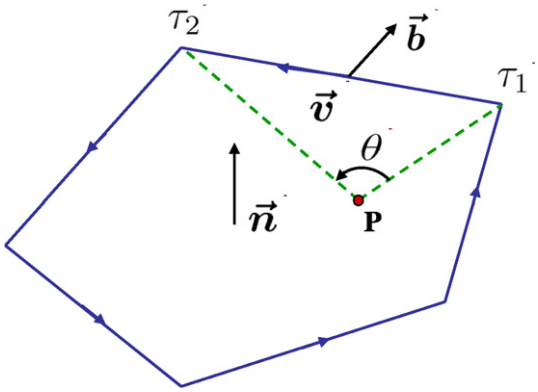

Fig. 1. Polygon representing a polyhedron face. Point P is the projection of the observation point on the polygon plane. Coordinate vectors satisfy the relation $\vec{\boldsymbol{b}}\times\vec{\boldsymbol{v}} = \vec{\boldsymbol{n}}$.

Let's consider an inclusion with a unit strain, $e = 1$, and with the shape of a right prism. The two base faces are normal to the z-axis while the lateral faces are parallel to the z-axis. Using above equations one finds the vertical stress tensor,

$$\sigma_{zz} = 2\mu\frac{1+\nu}{1-\nu}\left(\frac{\Omega_u + \Omega_l}{4\pi} - \delta_I\right). \tag{13}$$

Here, $\Omega_{u,l}$ are the solid angles subtended by the upper and lower base faces at the point of observation, $\delta_I = 0$ outside the inclusion and $\delta_I = 1$ inside the inclusion. Eq. (13) is a three-dimensional generalization of the expression derived by Downes et al. (1995) and Faux et al. (1997) for rectangular quantum wires.

In case of cuboidal inclusions, Eq. (13) is applicable to all three pairs of opposite faces. The sum of all solid angles vanishes outside the inclusion and it is equal to 4π inside the inclusion. One concludes that $\sigma_{ii} = 0$ outside and $\sigma_{ii} = -4\mu(1+\nu)/(1-\nu)$ inside the inclusion (Downes et al., 1997). These relations are valid for inclusions of arbitrary shapes, because they can be approximated by a collection of cuboidal inclusions.

In the limit where the number of sides of a prism tends to infinity, Eq. (13) becomes applicable to arbitrary cylindrical bodies whose cross-section is constant along the z-axis. The solid angle Ω_c subtended by a circle of radius r is equal to $\Omega_c = 2\pi[1 - d/(d^2 + r^2)^{1/2}]$. Here, d is the distance form the observation point to the circle center, and we consider points, which lay on the symmetry axis perpendicular to the circle plane. Applying Eq. (13) one finds that

$$\sigma_{zz} = -2\mu\frac{1+\nu}{1-\nu}\frac{h}{\sqrt{h^2 + 4r^2}} \tag{14}$$

in the cylinder center, where h is the cylinder height. Eq. (14) has been used to analyze stresses developing in formations due to extraction of hydrocarbons from oil and gas reservoirs (Kuvshinov, 2007a). The fluid pressure change p_f inside a reservoir has approximately a logarithmic profile,

$$p_f(r) = p_b\frac{\ln(r/r_d)}{\ln(r_b/r_d)}, \tag{15}$$

for $r_b < r < r_d$, and it is constant for $r < r_b$ and $r > r_d$. Here, r_b is the well bore radius, r_d is the radius of the drained area, and p_b is the fluid pressure drop near the well bore. The fluid pressure change p_f acts on the surrounding formation as an inclusion with a hydrostatic eigenstrain, whose amplitude is found by substituting Eq. (15) into Eq. (6). To calculate the vertical stress for an inclusion with a varying amplitude $e(r)$, one should integrate Eq. (14) with the weight $-\partial e/\partial r$. The corresponding integral can be found exactly. For the sake of clarity, we restrict ourself to the approximation, $r_b \ll h \ll r_d$, which is usually satisfied for real reservoirs. In this case

$$\frac{\sigma_{zz}}{p_b} = -\frac{1-2\nu}{1-\nu}\frac{\ln(h/r_b)}{\ln(r_d/r_b)}. \tag{16}$$

Parameter h in Eq. (16) represents the reservoir thickness. Eq. (16) turns out to be accurate enough for many practical purposes (Kuvshinov, 2007a). Although it has been derived under the assumption of an infinite and uniform formation, its predictions are very close to predictions of numerical codes, which take into account the full formation complexity.

3.3. Eshelby's tensor

Arbitrary (not necessarily hydrostatic) inclusions are conventionally described in terms of the Eshelby tensor S_{jkmn}, which relates the effective strain $e_{jk}^{(\mathrm{eff})}$ with the eigenstrain of the inclusion,

$$e_{ij}^{(\mathrm{eff})} = S_{ijkl}e_{kl}^{(I)}. \tag{17}$$

In an infinite and uniform medium it is equal to (Mura, 1987)

$$S_{ijkl} = \frac{1}{8\pi\mu(1-\nu)}\left[\Psi_{,ijkl} - 2\nu\Phi_{,ij}\delta_{kl} - (1-\nu)(\Phi_{,ik}\delta_{jl} + \Phi_{,il}\delta_{jk} + \Phi_{,jk}\delta_{il} + \Phi_{,jl}\delta_{ik})\right], \tag{18}$$

where $\Psi(\vec{r}) = \int_V R\mathrm{d}\vec{r}'$ is a bi-harmonic potential. Rodin (1996) has described an algorithm to calculate the potentials Φ and Ψ for polyhedral inclusions, and has calculated the Eshelby tensor in two dimensions. He concluded that in three-dimensions one should rely on symbolic computer algebra. Nozaki and Taya (2001) have managed to perform these calculations analytically, although they have finished with lengthy formulas. Our method leads to essentially simpler relations. The second order derivatives of the harmonic potential Φ are given by Eq. (11). The fourth order derivative of the bi-harmonic potential Ψ is calculated from Eqs. (A.3) and (A.16),

$$\Psi_{,ijkl} = 2n_in_j\Phi_{,kl} + \sum_{\text{polygons}} n_i \sum_{\text{edges}} \{b_jv_k[(n_lR_n + b_lR_b + v_lR_v)/R]|_{\tau_1}^{\tau_2} + [(b_jn_k + n_jb_k)R_n + (b_jb_k - n_jn_k)R_b]\left[v_l/R|_{\tau_1}^{\tau_2} - (n_lR_n + b_lR_b)I_{-3}\right] + [(b_jn_k + n_kb_j)n_l + (b_jb_k - n_jn_k)b_l]I_{-1}\}. \tag{19}$$

4. Hydrostatic inclusions in isotropic bi-materials

Hydrostatic inclusions in a semi-space have been originally studied by Mindlin and Cheng (1950) and Sen (1951). Below we consider a more general case of bi-materials (Rongved, 1955; Yu and Sanday, 1991; Yu et al., 1992; Tinti and Armigliato, 1998; Singh et al., 1999). The peculiarity of hydrostatic inclusions in bi-materials is that, similarly to inclusions in an infinite space, they are described by derivatives of Newtonian potential.

4.1. Green's functions

The displacement $\vec{u}^G$ induced by a delta-functional hydrostatic inclusion with $p^{(I)} = 1$, is described by the equation (Kuvshinov, 2007b)

$$\vec{u}^G = \frac{1}{4\pi H}\left[\nabla'\left(\phi^{(-)} + s_0\kappa\phi^{(+)} + s_0z\frac{\partial\phi^{(+)}}{\partial z'}\right) - 2\vec{e}_zs_0z\frac{\partial^2\phi^{(+)}}{\partial z'^2}\right], \tag{20}$$

which can be reconstructed from solution of Rongved (1955); Yu and Sanday (1991); Yu et al. (1992). Here, $\phi^{(\pm)} = 1/R_\pm$, $R_\pm = [(x'-x)^2 + (y'-y)^2 + (z' \pm z)^2]^{1/2}$,

$$s_0 = \frac{\mu - \mu_0}{\mu/2 + \kappa\mu_0}, \tag{21}$$

and $\kappa = (3-4\nu)/2$. Parameters without a subscript refer to the material containing inclusion, and μ_0 is the shear modulus of the other material. The case of a medium with a free boundary is recovered in the limit $\mu_0 \to 0$, which implies $s_0 = 2$. From Eq. (20) it follows that the displacement in bi-materials is related to displacement in an infinite region $\vec{u}^{(\infty)}$ as

$$\vec{u} = \vec{u}^{(\infty)} + s_0\kappa\vec{u}^{(+)} + s_0z\frac{\partial}{\partial z}\left(u_x^{(+)}, u_y^{(+)}, -u_y^{(+)}\right), \tag{22}$$

where $\vec{u}^{(+)}(x,y,z) = \vec{u}^{(\infty)}(x,y,-z)$. Eq. (22) holds for inclusions of arbitrary shapes, and it generalizes the relation given by Davies (2003). The displacement at the interface, $z = 0$, is equal to $\vec{u}(x,y,0) = [4(1-\nu) - (2-s_0)\kappa]\vec{u}^{(\infty)}(x,y,0)$. The displacement at the free surface is increased by a factor of $4(1-\nu) > 2$ compared to the displacement in an infinite medium. This is a known fact in geomechanics of hydrocarbon reservoirs (Geertsma, 1973), which has been rediscovered by Davies (2003).

The factor s_0 in Eq. (20) appears in front of terms with $\phi^{(+)}$. In the Mindlin and Cheng formalism (Mindlin and Cheng, 1950), such terms represent the "image" nucleus. Consequently, the elastic fields in bi-materials are obtained from corresponding expressions in a half-space, if one multiplies contributions of the image nuclei on $s_0/2$. We give the expression for the vertical stress, which is used in our further analysis (Kuvshinov, 2007b),

$$\sigma_{zz}^G = -\frac{\mu}{2\pi H}\frac{\partial^2}{\partial z'^2}\left(\phi^{(-)} - \frac{s_0}{2}\phi^{(+)} + s_0z\frac{\partial\phi^{(+)}}{\partial z'}\right) - \frac{2\mu}{H}\delta(\vec{r} - \vec{r}'). \tag{23}$$

4.2. Polyhedral inclusions

Eq. (23) contains a term with the third order derivative of $\phi^{(+)}$. This term is integrated using the relation

$$\int_V \phi_{,i'j'k'} \mathrm{d}\vec{\mathbf{r}}' = \sum_{\text{polygons}} n_i \sum_{\text{edges}} \left\{ \frac{b_j v_k}{R} \Big|_{\tau_1}^{\tau_2} - [(b_j n_k + n_j b_k) R_n + (b_j b_k - n_j n_k) R_b] I_{-3} \right\}, \tag{24}$$

which follows from Eqs. (A.3), (A.15). Eq. (24) together with Eqs. (10) and (11) provides a complete descriptions of elastic fields due to polyhedral inclusions in bi-materials. To integrate the value $\phi^{(+)}$ one uses the coordinate system $x_+ = x$, $y_+ = y$, $z_+ = -z$, where $\phi^{(+)}$ coincides with the standard Newtonian potential.

Fig. 2 shows the normalized vertical stress produced by a uniform tetrahedral inclusion, which has been calculated using above relations. The stress is normalized on the factor μ/H. For clarity we consider a half-space with the free-surface at $z = 0$. One face of the tetrahedron is a regular triangle inscribed in a unit circle laying in the plane $z = 0.3$. The coordinates of the tetrahedral top are equal $(0, 0, 1.7)$. The figure shows the stress levels in the vertical plane of symmetry $y = 0$. The vertical stress is continuous through the horizontal face. The stress has jumps at other faces. The level lines of the stress are continuous. This is a "geometric" continuity – lines corresponding to different values of the stress join smoothly at the inclusion boundary.

Arbitrary convex polyhedra can be represented as a combination of tetrahedra without gaps and overlaps. Consequently, the problem of polyhedral inclusions can be reduced to tetrahedral inclusions. The drawback of this approach is that it requires calculation of integrals, which cancel in the resulting expression. It might be preferable not to decompose polyhedra into tetrahedra, but to evaluate the volume integrals directly from general expressions.

4.3. Block-shaped inclusion

Let's calculate the vertical stress, σ_{zz}, due to a block-shaped inclusion and explain how to recover formulas reported by Hu (1989) and Glas (1991). The stress σ_{zz} (23) depends on the values $\Phi^{(\pm)}_{z'z'} = \int \phi^{(\pm)}_{z'z'} \mathrm{d}V$, and $\Phi^{(+)}_{z'z'z'} = \int \phi^{(+)}_{z'z'z'} \mathrm{d}V$, which are simplified to

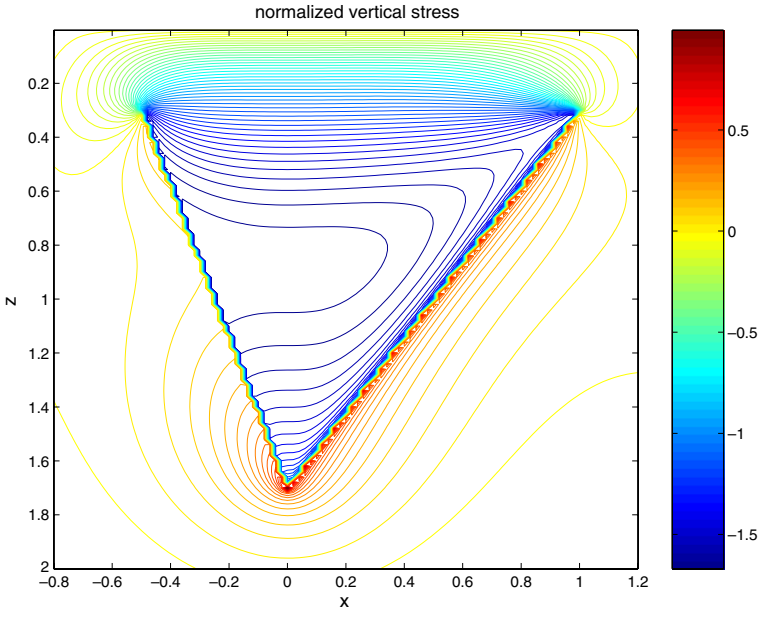

Fig. 2. Normalized vertical stress induced by a tetrahedral inclusion in half-space.

$$\Phi^{(\pm)}_{z'z'} = \sum_{\text{top,bottom}} n_z^2 \sum_{\text{edges}} \left(J_{-1} - \frac{R_n}{|R_n|}\theta \right), \quad \Phi^{(\pm)}_{z'z'z'} = \sum_{\text{top,bottom}} n_z^3 \sum_{\text{edges}} R_b I_{-3}. \tag{25}$$

Eq. (25) is valid for an arbitrary right prism, whose base lays in the horizontal (x,y)-plane. The summation there is carried out over two horizontal faces, which are denoted as "top" and "bottom". All the other faces do not contribute to σ_{zz}. We use the coordinate system where the vertical z-axis is directed downwards, so that the vertical coordinate of the "top" face z_{top} is smaller than the vertical coordinate of the "bottom" face z_{bottom}, $z_{\text{top}} < z_{\text{bottom}}$.

To find the sum over the "top" face of the inclusion, we label the vertices of this face as $i = 1, 2, 3, 4$ (see Fig. 3). The integrals J_{-1} and I_{-3} are calculated along the closed path $1 \to 2 \to 3 \to 4 \to 1$. Integration over the "bottom" face is performed similarly. Terms with θ in Eq. (25) vanish after integration for points laying outside the inclusion. Inside the block, their sum is equal to $2\mu/H$, which cancels the delta-functional term in Eq. (23).

Replacing the summation over edges by the summation over vertices we arrive at

$$\sigma_{zz} = -\frac{\mu}{2\pi H} \sum_{\text{vertices}} (-1)^{i-1} \left[\arctan\left(\frac{\zeta_- R_-}{\bar{x}\bar{y}} \right) - \frac{s_0}{2} \arctan\left(\frac{\zeta_+ R_+}{\bar{x}\bar{y}} \right) + s_0 z \frac{\bar{x}\bar{y}}{R_+} \left(\frac{1}{\bar{x}^2 + \zeta_+^2} + \frac{1}{\bar{y}^2 + \zeta_+^2} \right) \right]. \tag{26}$$

Here, $R_\pm = (\bar{x}^2 + \bar{y}^2 + \zeta_\pm^2)^{1/2}$, $\zeta_\pm = z_{(i)} \pm z$, $\bar{x}_{(i)} = x_{(i)} - x$, etc. and coordinates written with subscripts "(i)" refer to block vertices, where i is the vertex label. The sign of the factor $(-1)^{i-1}$ for different vertices is indicated in Fig. 3 by pluses and minuses.

Eq. (26) in a half-space coincides with the expression derived by Hu (1989) for points outside the inclusion. Glas (1991) has suggested that Hu's formula can be used inside the inclusion provided one adds there the term $p^{(I)}$ given by Eq. (6). According to Eq. (26), Hu's expression is applicable inside the inclusion if the term $-(2\mu/H)p\delta_{ij}$ is added to it, so that suggestion by Glas (1991) is incorrect. To confirm validity of Eq. (26) one can check that it provides continuity of σ_{zz} through the "top" and "bottom" boundaries of the inclusion. We have calculated σ_{zz} due to a block-shaped inclusion using general integral relations for polyhedra and using summation over vertices (26). In both cases the results were identical. The corresponding stress-field is shown in Fig. 4.

5. Extension of the method

Our previous analysis can be extended to treat analytically anisotropy effects, non-hydrostatic inclusions, and non-uniform inclusions. In addition, we give solutions to the Mindlin and Cherruti problems, and consider two-dimensional wires. In most cases we only outline the derivation procedure. We do not give all the resulting expressions, because they are rather bulky, although their derivation does not present conceptual difficulties.

5.1. Anisotropy effects

We consider hydrostatic deformations of a transversely isotropic space that represents a particular case of anisotropy. The properties of a transversely isotropic medium in a given direction depend only on the

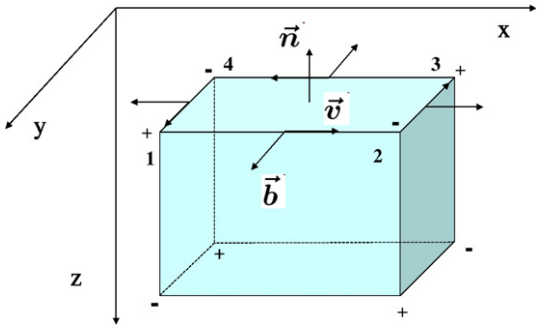

Fig. 3. Block-shaped inclusion in a half-space, "+" and "−" denote sign of the weight $(-1)^{i-1}$ in Eq. (26).

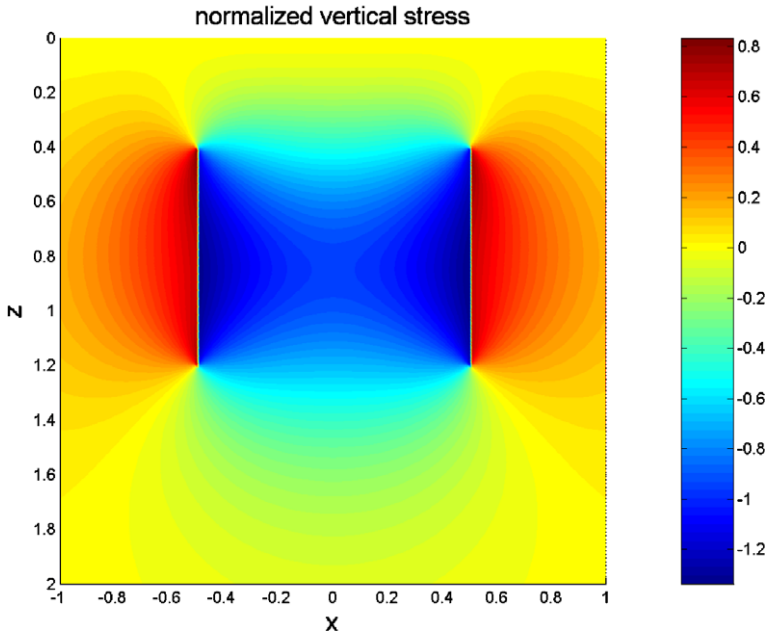

Fig. 4. Normalized stress σ_{zz} in the plane $y = 0$ induced by a parallelepiped-shape inclusion, $-0.5 < (x,y) < 0.5$, $0.4 < z < 0.8$. The plane $z = 0$ is the free surface.

angle between this direction and the symmetry axis. Crystals with hexagonal lattices provide an example of such a medium. We assume that the symmetry axis is $\vec{e}_z$, which corresponds to the choice of Miller indices $(0,0,1)$.

Green's functions in vertically isotropic bi-materials are given by Pan and Chou (1979b); Yu et al. (1995); Yu and Rath (2000). One can recover the required equations from these Green's functions by considering the limiting case of a center of dilatation. Alternatively, they can be derived using the reflectivity method of Kennett (1983), as it has been explained by Kuvshinov (2007b). The latter method is more general, because it is applicable to multi-layered media. It also leads to essentially more compact equations. The procedure described in Appendix B gives

$$\vec{u}_{\perp}^{G}(\vec{r}) = \frac{1}{2\pi B}\nabla'_{\perp}\left\{\lambda_{+}\left[\frac{a_{+}}{\widetilde{R}(-\lambda_{+},\lambda_{+})}+\frac{a_{11}}{\widetilde{R}(\lambda_{+},\lambda_{+})}+\frac{a_{21}}{\widetilde{R}(\lambda_{-},\lambda_{+})}\right]+\lambda_{-}\left[\frac{a_{-}}{\widetilde{R}(-\lambda_{-},\lambda_{-})}+\frac{a_{12}}{\widetilde{R}(\lambda_{+},\lambda_{-})}+\frac{a_{22}}{\widetilde{R}(\lambda_{-},\lambda_{-})}\right]\right\}, \tag{27}$$

$$u_{z}^{G}(\vec{r}) = \frac{1}{2\pi B}\frac{\partial}{\partial z'}\left\{q_{+}\left[\frac{a_{+}}{\widetilde{R}(-\lambda_{+},\lambda_{+})}-\frac{a_{11}}{\widetilde{R}(\lambda_{+},\lambda_{+})}-\frac{a_{12}}{\widetilde{R}(\lambda_{+},\lambda_{-})}\right]+q_{-}\left[\frac{a_{-}}{\widetilde{R}(-\lambda_{-},\lambda_{-})}-\frac{a_{21}}{\widetilde{R}(\lambda_{-},\lambda_{+})}-\frac{a_{22}}{\widetilde{R}(\lambda_{-},\lambda_{-})}\right]\right\}. \tag{28}$$

Here,

$$\tilde{R}(\pm\lambda_i,\lambda_j) = \left[(x-x')^2+(y-y')^2+(\pm\lambda_i z+\lambda_j z')^2\right]^{1/2}, \tag{29}$$

and constants B, $\lambda_{\pm}$, $a_{\pm}$, and $a_{1,2}$ are explained in Appendix B. Eqs. (27) and (28) reproduce Eq. (20) in the isotropic limit. Note, that transition to this limit is not trivial, because one needs to resolve uncertainties of the type "0/0".

Although Eqs. (27) and (28) look rather complicated, their underlying structure is simpler than the structure of correspondent isotropic equations. The coordinate dependence enters only through the modified radius $\widetilde{R}(\pm\lambda_i,\lambda_j)$. Stretching the horizontal coordinates as $(x,y)=\lambda_j(\tilde{x},\tilde{y})$ and placing the coordinate origin at the observation point, one transforms $\widetilde{R}(\pm\lambda_i,\lambda_j)$ to the Newtonian potential. After that one can integrate all the terms in Eqs. (27), (28) to find elastic fields produced by polyhedral inclusions.

Calculations based on Eqs. (27), (28) show that the anisotropy does not have an essential influence on elastic fields. This agrees with conclusions of Andreev et al. (1999). On the other hand, the anisotropy can change the pattern of the induced piezoelectric field. We study such effects in Section 6.

5.2. Non-hydrostatic inclusions

The Green tensor representing non-hydrostatic inclusions in an isotropic, uniform half-space is commonly written in a rather complicated form (Mura, 1987; Maranganti and Sharma, 2005; Ovid'ko and Sheinerman, 2005). The correspondent expression can be simplified to

$$G_{ij}(\vec{\boldsymbol{r}},\vec{\boldsymbol{r}}')=\frac{1}{16\pi\mu(1-\nu)}\left\{4(1-\nu)\left(\frac{1}{R_-}+\frac{1}{R_+}\right)\delta_{ij}-\frac{\partial^2}{\partial x_i'\partial x_j'}[R_-+(3-4\nu)R_+]\right.$$
$$\left.+2x_3\left[(3-4\nu)\left(\delta_{i3}\frac{\partial}{\partial x_j'}-\delta_{j3}\frac{\partial}{\partial x_i}\right)+x_3'\frac{\partial^2}{\partial x_i\partial x_j'}\right]\frac{1}{R_+}+4(1-\nu)(1-2\nu)\frac{\partial^2\chi_+}{\partial x_i'\partial x_j}\right\}. \tag{30}$$

Here, χ_+ is a harmonic potential,

$$\chi_+=(z+z')\ln(R_++z+z')-R_+. \tag{31}$$

The fact that the Green tensor admits representation of the form of Eq. (30) is intuitively obvious, because equilibrium of a semi-infinite body can be described in terms of the Galerkin vector, which is written as a combination of functions $R_\pm$ and χ_+ (Mindlin, 1936).

One can also derive Eq. (30) from the expression given by Yu and Sanday (1991) for elastic Green's tensor in an isotropic half-space. Expression by Yu and Sanday (1991) has a simple form, but it cannot be used directly for our analysis, because it contains non-harmonic functions of the type $x\ln(R_++z+z')$. One uses the circumstance that only derivatives of such non-harmonic functions appear in the equation for Green's tensor. Performing differentiation and rearranging terms, one obtains Eq. (30), which contains only powers of R and the harmonic potential χ_+ (31). Then one can make integration using the procedure of Appendices A and C.1. The term x_3'/R_+ is casted in the desired form straightforwardly, $x_3'/R_+=\partial R_+/\partial x_3'-x_3/R_+$. Elastic fields due to non-hydrostatic inclusions in bi-materials can be also expressed through the potentials $1/R_\pm$, $R_\pm$, $\chi_\pm$ (Mura, 1987), and hence can be integrated analytically.

5.3. Mindlin and Cherruti problems

The classical Mindlin and Cherruti problems deal with deformations of a semi-infinite solid induced by an interior or surface force $\vec{\boldsymbol{F}}$. One meets Cherruti problem also in analysis of piezoelectric effects in quantum dots (Davies et al., 1998). Usually one assumes that the force is applied to a single point. In this formulation the problem is reduced to calculation of the Green tensor. Much work has been done in the elasticity theory to calculate the Green tensor in a transversely isotropic (Chowdhury, 1987; Liao and Wang, 1998) and non-uniform (Wang et al., 2003) media. We restrict ourselves to a uniform isotropic half-space, where the Green tensor is given by Eq. (30).

The formal solution to the Mindlin and Cherruti problems is given by the integral

$$u_i(\vec{\boldsymbol{r}})=\int F_j(\vec{\boldsymbol{r}}')G_{ij}(\vec{\boldsymbol{r}},\vec{\boldsymbol{r}}')\mathrm{d}\vec{\boldsymbol{r}}', \tag{32}$$

where the integration is carried over the volume V or the surface S to which the force is applied. In contrast to Eq. (8), the Green tensor here is not differentiated. Integral (32) can still be found analytically as is explained in

Appendix C.2. As an illustration, we consider a unit vertical force F_z applied to a horizontal polygonal plate, which is buried at some depth. The normal surface displacement u_z due to this force is equal to

$$u_z = \frac{1}{4\pi\mu}\sum_{\text{edges}}[2(1-\nu)r_b I_{-1} + (1-2\nu)(r_n J_{-1} - |r_n|\theta)]. \tag{33}$$

Figs. 5 and 6 show results of calculations according to Eq. (33) for a star-shaped plate, buried in formation with $\nu = 0.25$. The shape effects are essential only at short distances. At distances larger than the characteristic size of the plate, the response is similar to the response from a point source.

5.4. Inclusions with non-uniform eigenstrain

If the inclusion strain has a linear dependence on the coordinate,

$$e_{ij}^{(I)} = e_{ij}^{(0)} + e_{ijk}^{(1)} x_k, \tag{34}$$

where $e_{ij}^{(0)}$ and $e_{ijk}^{(1)}$ are constant tensors, then in additions to previously calculated integrals one needs to integrate Green's functions with weights x_k'. The corresponding integrals have been calculated for ellipsoidal inclusions using the Ferrers and Dyson formula (Moschovidis and Mura, 1975; Mura, 1987). In this Section we explain how to perform such an integration over polyhedra. We consider hydrostatic inclusions only.

For our purpose we need to express functions of the type $r^n x_i x_j \ldots$ through derivatives of r^n and then use equations of Appendix A. We start from the relations $\nabla r^n = n r^{n-2}\vec{\boldsymbol{r}}$ and $\nabla \otimes \vec{\boldsymbol{r}} = \vec{\boldsymbol{e}}_i \otimes \vec{\boldsymbol{e}}_i$, where $\otimes$ is the sign of the tensor multiplication as in Appendix A. Applying the operator $\nabla\otimes$ to these relations recursively one finds

$$\frac{\nabla \otimes \nabla r^n}{n} = r^{n-2}\vec{\boldsymbol{e}}_i \otimes \vec{\boldsymbol{e}}_i + (n-2)r^{n-4}\vec{\boldsymbol{r}} \otimes \vec{\boldsymbol{r}}, \tag{35}$$

$$\frac{\nabla \otimes \nabla \otimes \nabla r^n}{n(n-2)} = r^{n-4}\sum\{\vec{\boldsymbol{r}} \otimes \vec{\boldsymbol{e}}_i \otimes \vec{\boldsymbol{e}}_i\} + (n-4)r^{n-6}\vec{\boldsymbol{r}} \otimes \vec{\boldsymbol{r}} \otimes \vec{\boldsymbol{r}}, \tag{36}$$

$$\frac{\nabla \otimes \nabla \otimes \nabla \otimes \nabla r^n}{n(n-2)} = r^{n-4}\sum\{\vec{\boldsymbol{e}}_j \otimes \vec{\boldsymbol{e}}_j \otimes \vec{\boldsymbol{e}}_i \otimes \vec{\boldsymbol{e}}_i\} + (n-4)\left[r^{n-6}\sum\{\vec{\boldsymbol{r}} \otimes \vec{\boldsymbol{r}} \otimes \vec{\boldsymbol{e}}_i \otimes \vec{\boldsymbol{e}}_i\} + (n-6)r^{n-8}\vec{\boldsymbol{r}} \otimes \vec{\boldsymbol{r}} \otimes \vec{\boldsymbol{r}} \otimes \vec{\boldsymbol{r}}\right]. \tag{37}$$

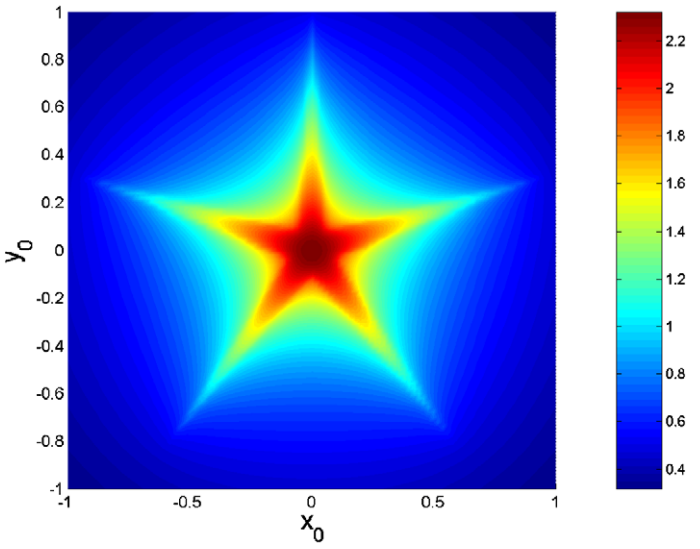

Fig. 5. Normalized surface displacement due to a unit vertical force applied to a horizontal star-shaped plate. The outer and inner star radii are 1 and 0.1, and the plate is buried at an infinitesimally small depth.

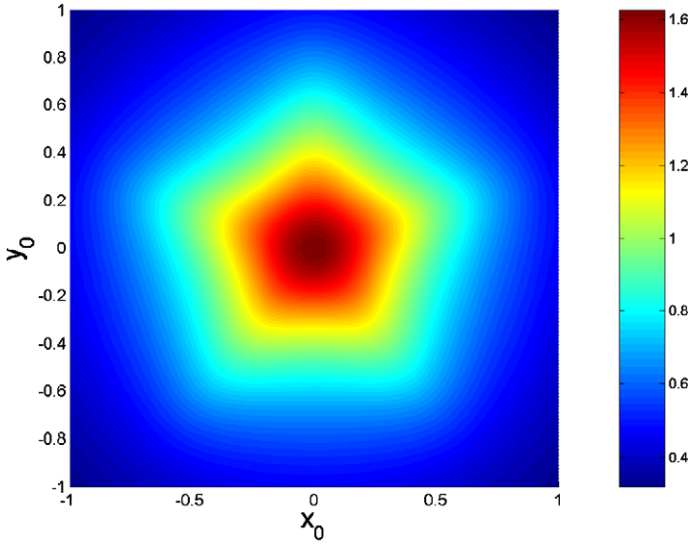

Fig. 6. The same as Fig. 5 with the plate buried at depth 0.2.

The curly brackets $\{\cdots\}$ in Eqs. (36) and (37) denote all different permutations of distinguishable vectors. For example, the sum $\sum\{\vec{r}\otimes\vec{r}\otimes\vec{e}_i\otimes\vec{e}_i\}$ contains six terms, since every arrangement is determined by positions of two vectors $\vec{r}$, and hence the number of distinguishable combinations is equal to $C(4,2)=6$. The sum $\sum\{\vec{e}_j\otimes\vec{e}_j\otimes\vec{e}_i\otimes\vec{e}_i\}$ contains three terms: the indices "i" and "j" are dumb, and we do not distinguish their interchanging $i\leftrightarrow j$. Eqs. (35)–(37) allow to express values $r^n\vec{r}\otimes\ldots\otimes\vec{r}$ through combinations $\nabla\otimes\ldots\otimes\nabla r^n$ that have been integrated in Appendix A.

Combinations of the type $\vec{r}\otimes\cdots\otimes\vec{r}/r$ appear when one calculates the Newtonian potential $\int(\rho_e/r)\mathrm{d}V$ produced by bodies with densities $\rho_e(\vec{r})$ varying according to a polynomial law, $\rho_e=c^{(0)}+c_i^{(1)}r_i+c_{ij}^{(2)}x_ix_j+\cdots$. Analytical expressions for the Newtonian potential produced by polyhedra with linear density have been presented by Pohánka (1998); Hansen (1999); Holstein (2003). Densities with a quadratic and cubic dependence on one of the coordinates have been analyzed by Gallardo-Delgado et al. (2003) and García-Abdeslem (2005) for the case of right rectangular prisms. Our equations provide analytical formulas for the Newtonian potential of polyhedra whose density is an arbitrary polynomial of the fourth degree.

Inclusions with an arbitrary eigenstrain, can be approximated by piece-wise linear inclusions, similarly to what is done in finite-element codes. One splits the space into tetrahedral cells and specifies the values of the eigenstrain in the vertices. The eigenstrain tensor inside each of the tetrahedra can be chosen in the from of Eq. (34). For each component $e_{ij}^{(I)}$ one can adjust the four arbitrary constants $e_{ij}^{(0)}$ and $e_{ijk}^{(1)}$ with $k=1,2,3$ in such a way, that $e_{ij}^{(I)}$ has the specified values in the four vertices of the tetrahedron. Summing contributions from separate tetrahedra one obtains the total elastic field. The resulting eigenstrain field will be continuous everywhere. Thus, a linear finite-element analysis of inclusions in bi-materials can be done analytically.

5.5. Quantum wires

Formally, we have already derived the two-dimensional quantum wire solution. It can be viewed as the limiting case of our formulas, where the inclusion has an infinitely large extension in one direction. However, general equations in this limit contain infinitely large terms canceling each other. For this reason, it is more convenient to make the transition to the two-dimensional case analytically, similarly to what is done in the gravity theory (MacMillan, 1930).

We assume that the wire is aligned along the y-axis, and integrate the potentials $1/R_\pm$, $R_\pm$, and χ_+ in the y-direction from $-y_0$ to y_0, where y_0 is a large value. Neglecting constants of integration, which disappear when the Green tensor is differentiated according to Eq. (8), we obtain the two-dimensional counterparts of the above potentials,

$$\phi = -2\ln\rho, \quad \psi = -\rho^2\ln\rho,$$
$$\chi = (x^2 - z^2)\ln\rho - 2xz\arctan\frac{z}{x}, \tag{38}$$

where $\rho = (x^2 + z^2)^{1/2}$. The potential χ in Eq. (38) is a harmonic function, which is equal to the real part of the complex function $\xi\ln\xi$, with $\xi = x + i\,z$.

Since elastic deformations are determined by derivatives of potentials, it is sufficient to use Eqs. (A.12) and (A.14). Derivatives along the vector $\vec{\boldsymbol{n}}$ are absent in the two dimensional case. Making the substitution $F = \nabla f$, we have

$$\int\int_{\text{polygon}} \nabla\otimes\nabla\otimes\nabla f\,\mathrm{d}S = \sum_{\text{edges}} \vec{\boldsymbol{b}}\otimes\left[\vec{\boldsymbol{v}}\otimes\nabla f\big|_{\tau_1}^{\tau_2} - \vec{\boldsymbol{b}}\otimes(\vec{\boldsymbol{n}}\times\nabla f)\big|_{\tau_1}^{\tau_2} + \vec{\boldsymbol{b}}\otimes\vec{\boldsymbol{b}}\int\nabla^2 f\,\mathrm{d}r_v\right]. \tag{39}$$

Setting $f = \phi$, ψ, χ one calculates the required integrals. In particular,

$$\int\int(\ln\rho)_{,ij}\mathrm{d}S = \sum_{\text{edges}} b_i(v_j\ln\rho + b_j\theta)\big|_{\tau_1}^{\tau_2}, \tag{40}$$

$$\int\int\psi_{,ijkl}\mathrm{d}S = \sum_{\text{edges}}\{b_i[v_j\psi_{,kl} + b_j(v_k b_m - b_k v_m)\psi_{,ml} - 4b_j b_k(v_l\ln\rho + b_l\theta)]\}\big|_{\tau_1}^{\tau_2}. \tag{41}$$

Eqs. (40) and (41) are sufficient to determine the Eshelby tensor in an infinite space.

Notice an analogy between Eqs. (12) and (40). Eq. (12) contains the solid angle Ω subtended by the surface, and Eq. (40) contains the edge apex angle θ. Following the discussion of Section 3.2, one concludes that the diagonal components of the stress tensor in directions perpendicular to the boundaries of a rectangular wire are determined by the sum of apex angles of two opposite boundaries (Downes et al., 1995).

6. Piezoelectric fields

The piezoelectric fields in quantum dots have been calculated both numerically (Grundmann et al., 1995; Jogai, 2001) and analytically (Larkin et al., 1997; Williams et al., 2004, 2005). Davies (1998, 1999) has derived simple equations for spherical and cuboidal dots in a uniform infinite medium. More sophisticated approaches have been developed by Pan, who has analyzed the anisotropy effects (Pan, 2002c) and introduced a fully coupled model (Pan, 2002a), where not only does the elastic stress generate a piezoelectric field, but also the piezoelectric field influences the stress–strain relation. The model of Pan (2002a) has been used to investigate a semi-infinite anisotropic medium (Pan, 2002b; Pan and Yang, 2003). Wang et al. (2006) have analyzed the case of an arbitrary anisotropy. In order to calculate the required integrals, Wang et al. (2006) approximated arbitrary surfaces by a set of triangles, which is essentially the same as the approach suggested by Rodin (1996).

Results by Pan (2002a,b); Pan and Yang (2003) refer to a point quantum dot, and they have been derived in the Fourier space, except for the case of an isotropic medium with a conducting surface. In order to analyze finite size effects one needs to use the inverse 2D Fourier transform and then perform an additional three-dimensional integration. An alternative approach has been suggested by Williams et al. (2004, 2005), who reduced calculation of piezo-electric field to calculation of surface integrals. This simplification was possible, because Williams et al. (2004, 2005) considered an elastically anisotropic infinite space. Still, the resulting surface integrals have not been found explicitly.

In this Section we derive fully analytical, algebraic relations for piezoelectric fields induced by cuboidal quantum dots in bi-materials. It is also explained how to obtain the corresponding relations for polyhedral dots. We restrict ourselves to a semi-coupled model, which according to Pan (2002a) is accurate enough for GaAs.

6.1. Strain-induced potential

Strains in a solid medium induce an electric polarization with the dipole momentum per unit volume $\vec{\boldsymbol{P}} = d_{ijk}e_{jk}^{(\text{eff})}$. Here, d_{ijk} is the piezoelectric tensor. The correspondent electric displacement vector is given

by $\vec{\boldsymbol{D}} = \epsilon\vec{\boldsymbol{E}} + 4\pi\vec{\boldsymbol{P}}$, where $\vec{\boldsymbol{E}}$ is the electric field, and ϵ is the intrinsic dielectric constant of the medium. In the static case, the electric field is determined by the scalar piezoelectric potential φ, $\vec{\boldsymbol{E}} = -\nabla\varphi$. If external electric charges are absent, then the electric displacement vector satisfies the equation $\nabla\cdot\vec{\boldsymbol{D}} = 0$, which reduces to

$$\nabla^2\varphi = \frac{4\pi}{\epsilon}\nabla\cdot\vec{\boldsymbol{P}}. \tag{42}$$

Solution of Eq. (42) is written as $\varphi = \varphi_{\Pi} + \varphi_b$. Here, φ_{Π} is a particular solution and φ_b is a harmonic potential, which is chosen to satisfy the condition at the interface.

One can express φ_{Π} through the vector pseudopotential $\vec{\boldsymbol{\Pi}}$: $\varphi_{\Pi} = (4\pi d_{ijk}/\epsilon)\Pi_{k,\,ij}$, which is defined as a non-singular solution of the equation $\nabla^2\vec{\boldsymbol{\Pi}} = \vec{\boldsymbol{u}}$ (Davies et al., 1998). The vector pseudopotential for isotropic half-space is found by integrating the Green tensor (30) taking into account the expressions $\nabla^2 r = 2/r$, $\nabla^2 r^3 = 12r$, and $\nabla^2[3(\vec{\boldsymbol{a}}\cdot\vec{\boldsymbol{r}})^2\chi - r^3] = 18\chi$. In case of hydrostatic inclusions in a transversely isotropic media, one needs to integrate values $\widetilde{R}(\pm\lambda_i,\lambda_j)$ (29). To perform this integration, we introduce the function $\chi(\pm\lambda_i,\lambda_j)$,

$$\chi(\pm\lambda_i,\lambda_j) = (\pm\lambda_i z + \lambda_j z')\ln[\widetilde{R}(\pm\lambda_i,\lambda_j) \pm \lambda_i z + \lambda_j z'] \pm \lambda_i z + \lambda_j z'. \tag{43}$$

One can check that $\nabla^2\chi(\pm\lambda_i,\lambda_j) = (\lambda_i^2 - 1)/\widetilde{R}(\pm\lambda_i,\lambda_j)$, which leads to

$$\nabla^2\frac{\chi(\pm\lambda_i,\lambda_j) - \bar{\chi}(\pm\lambda_i,\lambda_j)}{\lambda_i^2 - 1} = \frac{1}{\widetilde{R}(\pm\lambda_i,\lambda_j)}. \tag{44}$$

Here, $\bar{\chi}(\pm\lambda_i,\lambda_j)$ is a harmonic function, which is obtained from $\chi(\pm\lambda_i,\lambda_j)$ by stretching the horizontal coordinates as $(x,y)\to\lambda_i(x,y)$. The function $\bar{\chi}(\pm\lambda_i,\lambda_j)$ is introduced to avoid non-physical singularities that would represent external charges.

6.2. Isotropic cubic lattices

Cubic lattices are characterized by three independent Voigt constants: $C_{11} = C_{22} = C_{33}$, $C_{12} = C_{13} = C_{23}$, and $C_{44} = C_{55} = C_{66}$. In this Section we consider a particular case, where the above constants are related by the isotropic condition $C_{11} = C_{12} + 2C_{66}$.

6.2.1. Particular solution

The piezoelectric tensor d_{ijk} for crystals with cubic lattices has six non-zero elements with $i\neq j\neq k$. All these elements are equal to d_{14}, so that $\vec{\boldsymbol{P}} = 2d_{14}(e_{yz}\vec{\boldsymbol{e}}_x + e_{xz}\vec{\boldsymbol{e}}_y + e_{xy}\vec{\boldsymbol{e}}_z)$, and Eq. (42) reduces to

$$\nabla^2\varphi = \frac{6d_{14}}{\epsilon H}\frac{\partial^3}{\partial x'\partial y'\partial z'}\left[\frac{1}{R_-} + \frac{s_0(1-\kappa)}{3R_+} + s_0 z'\frac{\partial}{\partial z'}\frac{1}{R_+} - s_0\frac{\partial^2 R_+}{\partial z'^2}\right]. \tag{45}$$

Integrating Eq. (45) we find

$$\varphi_{\Pi} = \frac{3d_{14}}{\epsilon H}\frac{\partial^2}{\partial x'\partial y'}\left[\frac{z'-z}{R_-} + \frac{s_0(1-\kappa)}{3}\frac{z'+z}{R_+} + \frac{s_0}{2}\frac{z'-z}{R_+} + \frac{s_0}{2}\left(z'^2 - z^2\right)\frac{\partial}{\partial z'}\frac{1}{R_+}\right]. \tag{46}$$

We have performed the differentiation with respect to z' explicitely, since form (46) is convenient to analyze conditions at interface.

6.2.2. Conducting interface

If the interface is conducting, then $\varphi = \varphi^{(\mathrm{cond})} = 0$ at $z = 0$, which is satisfied for

$$\varphi_b^{(\mathrm{cond})} = -\frac{3d_{14}}{\epsilon H}\frac{\partial^2}{\partial x'\partial y'}\left[\frac{z'}{R_+} + \frac{s_0(1-\kappa)}{3}\frac{z'}{R_+} + \frac{s_0}{2}\frac{z'}{R_+} + \frac{s_0 z'^2}{2}\frac{\partial}{\partial z'}\frac{1}{R_+}\right]. \tag{47}$$

Eqs. (46) and (47) coincide with equations by Pan (2002a) for a traction-free interface. Combining Eqs. (46) and (47) and performing the integration with respect to z' we find

$$\varphi^{(\mathrm{cond})} = \frac{3d_{14}}{\epsilon H}\frac{\partial^3}{\partial x'\partial y'\partial z'}\left\{R_- - R_+ + \left[1 - \frac{s_0}{2} + \frac{s_0(1-\kappa)}{3}\right]z\frac{\partial \chi_+}{\partial z'} - \frac{s_0 z^2}{2R_+}\right\}. \tag{48}$$

Eq. (48) reproduces the result by Davies (1998) in the limit of an infinite medium. Eq. (48) can be integrated to give the piezoelectric potential induced by arbitrary polygonal inclusions. The integration is trivial for the case of parallelepiped-shaped inclusions, where the resulting piezoelectric potential is obtained by summing the expression standing in curly brackets over the vertices of the parallelepiped with alternating signs.

Fig. 7 shows the electric potential in the plane $y = 0.5$ and the vertical electric field at the interface induced by a parallelepiped-shaped inclusion. The piezoelectric potential and the electric field have an octuple struc-

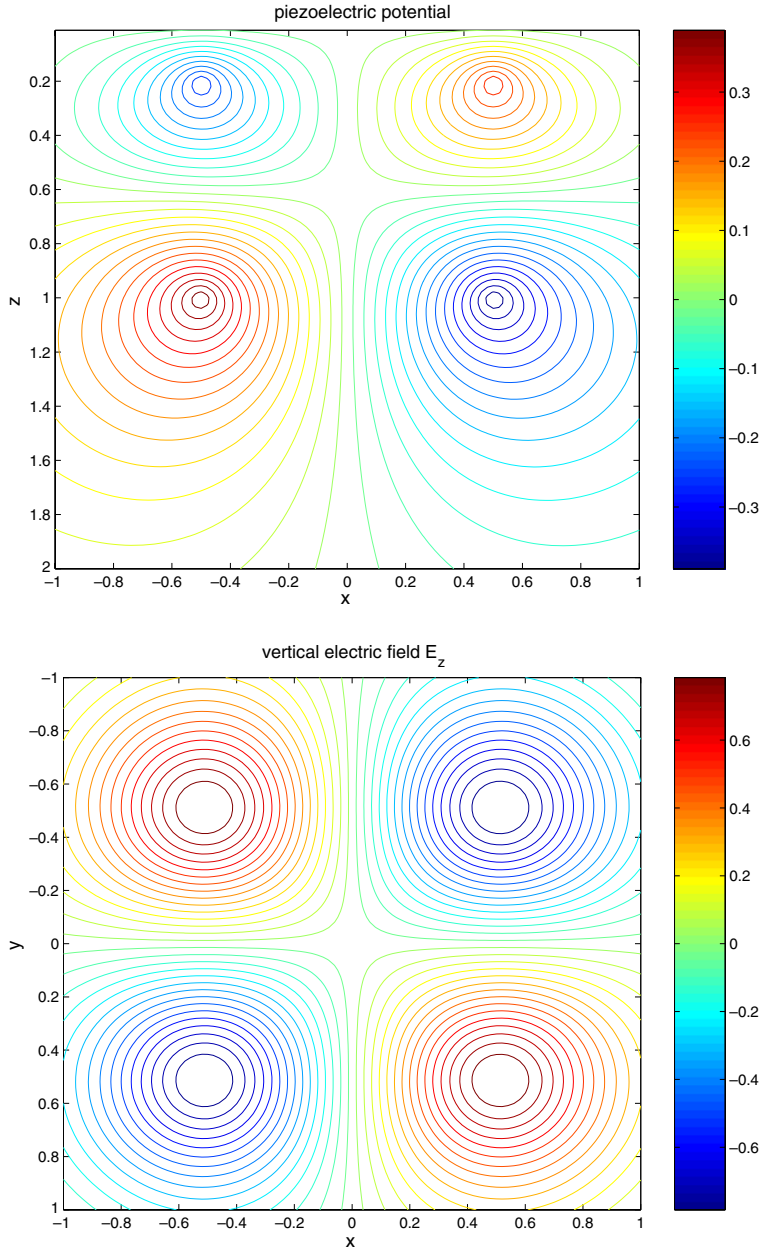

Fig. 7. Piezoelectric potential and contours of the vertical electric field due to a parallelepiped-shaped inclusion (the same as in Fig. 4) in a half-space with conducting surface and $\nu = 0.25$. The values are normalized on the factor $d_{14}/(\epsilon H)$.

ture. Maxima and minima are located near the positions of vertices. The same pattern has been observed by Pan (2002a).

6.2.3. Insulating interface

The boundary condition for an insulating interface reads as $D_z = 0$, or $\partial\varphi_b/\partial z = \partial\varphi_b^{(\mathrm{ins})}/\partial z = -\partial\varphi_{\Pi}/\partial z + (4\pi/\epsilon)P_z$ at $z = 0$. Pan (2002a) has expressed the corresponding potential $\varphi_b^{(\mathrm{ins})}$ in terms of double Fourier integrals. We see however that the potential $\varphi_b^{(\mathrm{ins})}$ admits an analytical representation,

$$\varphi_b^{(\mathrm{ins})} = \frac{d_{14}}{\epsilon H}\frac{\partial^2}{\partial x'\partial y'}\left\{\frac{3z'}{R_+} - \frac{s_0(5-2\kappa)z'}{2R_+} + \left[1+\frac{s_0}{2}(1-2\kappa)\right]\frac{\partial\chi_+}{\partial z'} - \frac{3s_0}{2}z'^2\frac{\partial}{\partial z'}\frac{1}{R_+}\right\}. \tag{49}$$

Combining Eqs. (46), (49) and performing another integration with respect to z', we find the full potential

$$\varphi^{(\mathrm{ins})} = \frac{d_{14}}{\epsilon H}\frac{\partial^3}{\partial x'\partial y'\partial z'}\left\{3(R_- + R_+) - \left[3+\frac{s_0}{2}(1+2\kappa)\right]z\frac{\partial\chi_+}{\partial z'} + \left[1+\frac{s_0}{2}(1-2\kappa)\right]\chi_+ - \frac{3s_0z^2}{2R_+}\right\}. \tag{50}$$

Fig. 8 shows the piezoelectric potential and the horizontal electric field $E_h = \sqrt{E_x^2 + E_y^2}$ produced by a parallelepiped-shaped inclusion at the insulating surface. The geometry and normalizations are the same as in Fig. 7. The resulting fields agree with calculations of Pan (2002b) for quantum dots in GaAs (0, 0, 1). Fig. 9 shows piezoelectric fields due to a cuboidal inclusion with unit length, whose diagonal is perpendicular to the interface. The piezoelectric fields are similar to those found by Pan (2002b) for a quantum dot buried in GaAs (1, 1, 1).

6.3. Anisotropy effects in cubic lattices

In this Section we consider the substrate GaAs (0, 0, 1), whose elastic moduli are equal to $B = C_{11} = 118\times10^9$ N/m^2, $G = C_{66} = 59\times10^9$ N/m^2, and $F = C_{13} = 54\times10^9$ N/m^2. One can model this lattice by specifying the elastic constants C_{66} and $C_{12} = C_{13}$, and then calculating C_{11} from the isotropic condition $C_{11} = C_{12} + 2C_{66} = 172\times10^9$ N/m^2. Such an approach however predicts incorrect values of elastostatic strains (Pan and Yang, 2001) and incorrect patterns of piezoelectric fields (Pan, 2002b). We propose an alternative method of modeling, where a cubic lattice is approximated by a vertically isotropic medium. Namely, we treat B, G, and F as three independent parameters. We also use the conditions $C_{11} = C_{22} = C_{33}$, $C_{13} = C_{23}$, and $C_{44} = C_{55} = C_{66}$, which are satisfied for cubic lattices. In contrast to actual cubic lattices, the parameter C_{12} is not equal to C_{13}, and it is found from the relation $C_{12} = C_{11} - 2C_{66}$, which holds also for transversely isotropic media. Calculations given below show that the method proposed gives qualitatively the same results as rigorous modeling (Pan, 2002b).

Substituting Eqs. (27) and (28) into Eq. (42) one finds that the piezoelectric potential in a transversely isotropic medium satisfies the equation

$$\nabla^2\varphi = \frac{4d_{14}}{\epsilon B}\frac{\partial^3}{\partial x'\partial y'\partial z'}\left\{(q_+ + 2\lambda_+)\left[\frac{a_+}{\widetilde{R}(-\lambda_+,\lambda_+)} - \frac{a_{11}}{\widetilde{R}(\lambda_+,\lambda_+)} - \frac{a_{12}}{\widetilde{R}(\lambda_+,\lambda_-)}\right] + (q_- + 2\lambda_-)\left[\frac{a_-}{\widetilde{R}(-\lambda_-,\lambda_-)} - \frac{a_{21}}{\widetilde{R}(\lambda_-,\lambda_+)} - \frac{a_{22}}{\widetilde{R}(\lambda_-,\lambda_-)}\right]\right\}. \tag{51}$$

Each of the terms proportional to $1/\widetilde{R}(\pm\lambda_i,\lambda_j)$ is integrated using Eq. (44), which gives the function φ_{Π}.

The function $\chi(1,\lambda_j)$ is harmonic and at $z = 0$ it coincides with $\chi(\pm\lambda_i,\lambda_j)$. Consequently, the boundary condition on a conductive interface is satisfied if one sets $\chi(\pm\lambda_i,\lambda_j) \to \chi(\pm\lambda_i,\lambda_j) - \chi(1,\lambda_j)$ in Eq. (44). One should also make the substitution $\bar{\chi}(\pm\lambda_i,\lambda_j) \to \bar{\chi}(\pm\lambda_i,\lambda_j) - \bar{\chi}(\lambda_i,\lambda_j)$ to ensure absence of singularities along the axis $x - x' = 0$ and $y - y' = 0$.

The vertical component of the dipole momentum P_z is equal to

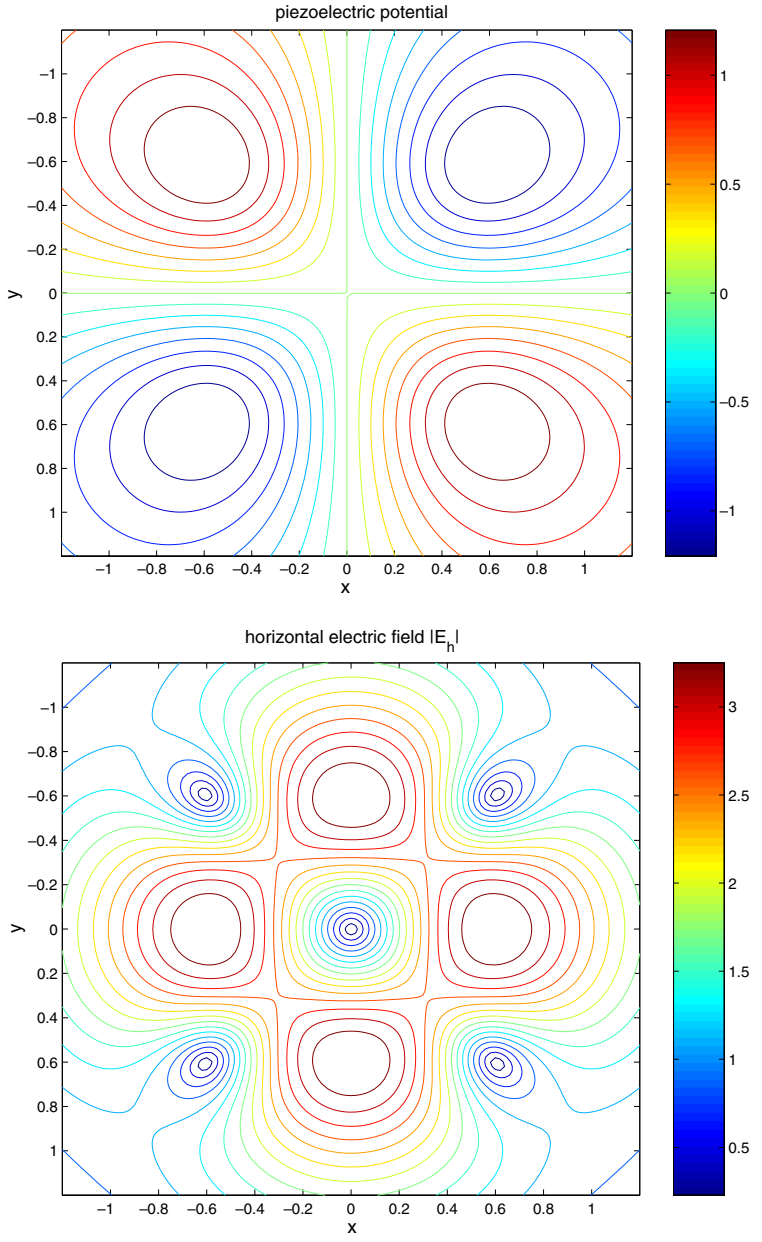

Fig. 8. Piezoelectric potential and horizontal electric field at $z = 0$ due to a parallelepiped-shaped inclusion in a half-space with insulating surface.

$$\frac{4\pi}{\epsilon}P_z = \frac{4d_{14}}{\epsilon B}\frac{\partial^4}{\partial x'\partial y'\partial z'\partial z}\left\{\frac{1}{\lambda_+}[a_+\chi(-\lambda_+,\lambda_+) - a_{11}\chi(\lambda_+,\lambda_+) - a_{12}\chi(\lambda_+,\lambda_-)] + \frac{1}{\lambda_-}[a_-\chi(-\lambda_-,\lambda_-) - a_{21}\chi(\lambda_-,\lambda_+) - a_{22}\chi(\lambda_-,\lambda_-)]\right\}. \tag{52}$$

From Eqs. (44), (51), (52) one sees that the value $D_z = -\partial\,\varphi_{II}/\partial z + (4\pi/\epsilon)P_z$ is a sum of fourth order derivatives with respect to x', y', z', and z of some expressions, symbolically written as $(\ldots)$. The brackets $(\ldots)$ contain terms proportional to $\chi(\pm\ \lambda_i,\lambda_j)$ and $\bar{\chi}(\pm\lambda_i,\lambda_j)$. Since $\partial\chi(\pm\lambda_i,\lambda_j)/\partial z \propto \pm\,\lambda_i$, the substitutions $\chi(\pm\lambda_i,\lambda_j) \to \chi(\pm\lambda_i,\lambda_j) \mp \lambda_i\chi(1,\ \lambda_j)$ and $\bar{\chi}(\pm\lambda_i,\lambda_j) \to \bar{\chi}(\pm\lambda_i,\lambda_j) \mp \bar{\chi}(\lambda_i,\lambda_j)$ in above brackets result in the solution for an insulated interface.

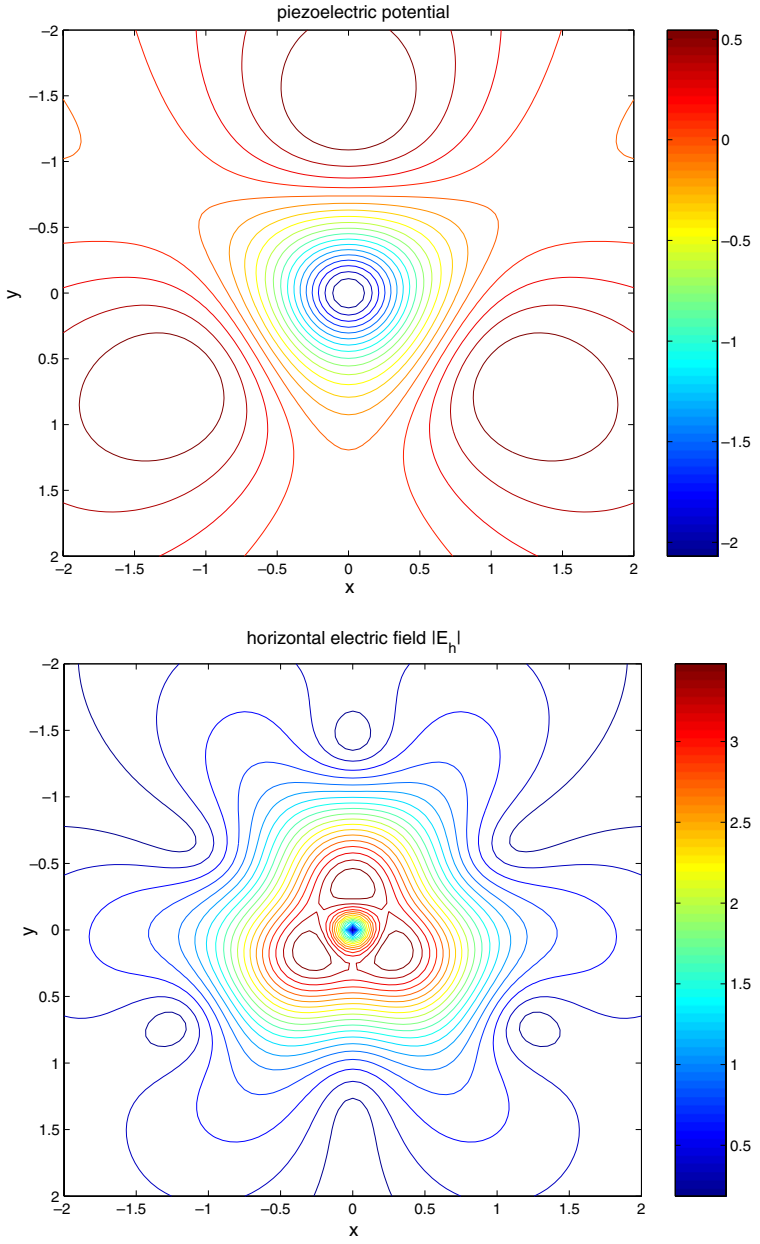

Fig. 9. Piezoelectric potential and contours of the horizontal electric field at $z = 0$ due to a cuboidal inclusion in a half-space with insulating surface. The cube diagonal is perpendicular to the surface.

The vertical electric field at an insulating interface is equal to $E_z = -(4\pi/\epsilon P_z)$. To calculate E_z for a cuboidal inclusion, one sums the expression in curly brackets in Eq. (52) over the vertices. Fig. 10 shows the result of this calculation. The same pattern as in the left side of Fig. 10 has been obtained by Pan (2002b), who calculated piezoelectric fields due to buried quantum dots. A deeply buried cube produces practically the same field at the interface as a dot. When the size of inclusion is comparable to its depth, then the difference with the dot becomes visible. When the cube lays close to the surface, then the central circle in Fig. 10 disappears, and the pattern becomes topologically the same as in the isotropic case. This example shows that the approximation of a point-wise inclusion can fail to describe the interface effects adequately.

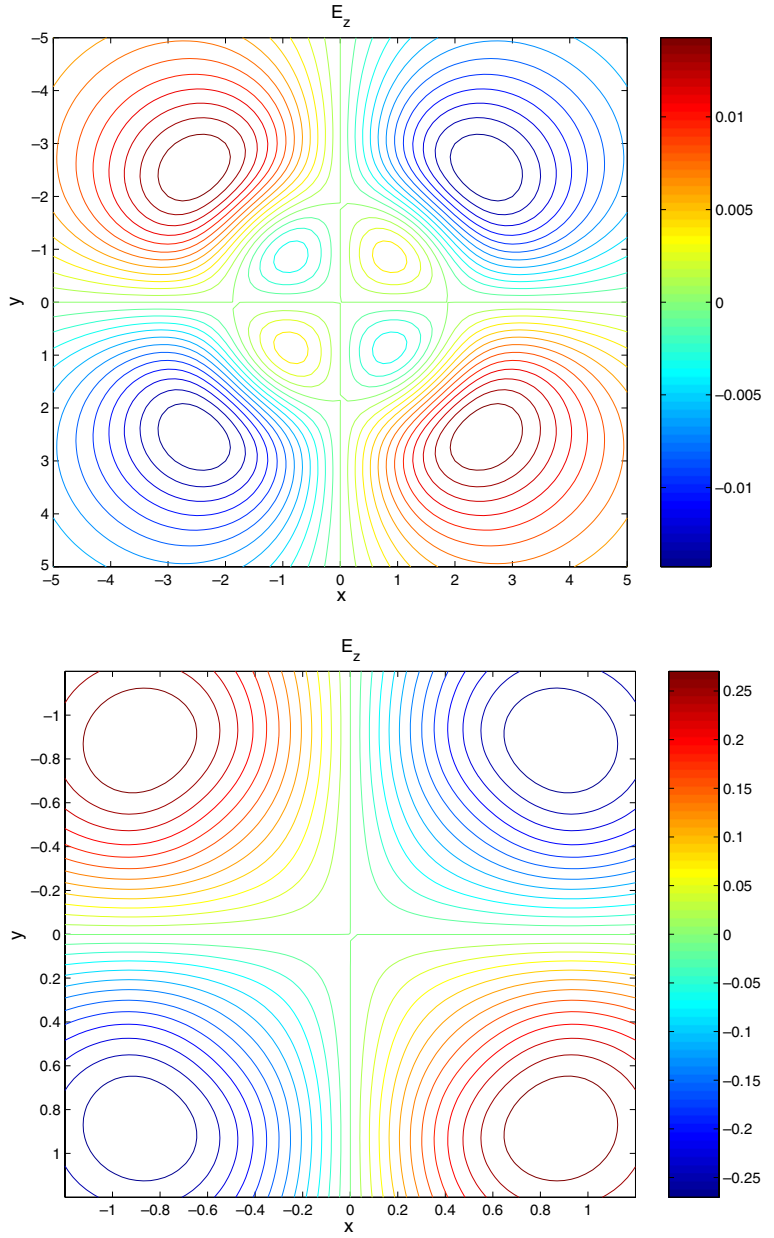

Fig. 10. Normalized vertical electric field, $E_z/(4d_{14}/B)$, at an insulating interface produced by a unit cuboidal inclusion. The top face of the cube is buried at depth 2.5 (upper figure) and at depth 0.1 (lower figure). The value E_z is normalized on the factor $4d_{14}/B$.

6.4. Nitride-based dots

Nitride alloys generally possess hexagonal lattices. The piezoelectric as well as elastic structure of such lattices is transversely isotropic. If the symmetry axis is in the z-direction, then the non-vanishing components of the piezoelectric tensor are equal to $d_{113} = d_{223} = d_{15}$, $d_{311} = d_{322} = d_{31}$, $d_{333} = d_{33}$ (Williams et al., 2004; Pan, 2002a), and

$$\nabla \cdot \vec{\boldsymbol{P}} = d_{31} \frac{\partial \nabla \cdot \vec{\boldsymbol{u}}}{\partial z} + d_{15} \nabla_{\perp}^2 u_z + (d_{33} - d_{31}) \frac{\partial^2 u_z}{\partial z^2}. \tag{53}$$

Eq. (42) reduces in the case considered to the form of Eq. (51), and it is solved in the same way. The difference with the cubic lattices is that one meets double differentiations with respect to same coordinates. To integrate

the resulting expressions one should use equations of Appendices A, C even for cuboidal inclusions. One should also have in mind that the piezoelectric field is strong in nitride alloys, and hence a semi-coupled model might be inadequate (Pan, 2002a).

7. Conclusions

We have considered misfitting inclusions in uniform semi-space and bi-materials, which can possess a transverse isotropy. Analysis of deformations induced by such inclusions is reduced to calculation of integrals containing harmonic and higher harmonic functions and their derivatives. In case of uniform polyhedral inclusions, we have expressed the correspondent integrals through algebraic functions. This provides a fully analytical description of the induced deformations.

The above result allows to solve exactly a number of problems in physics and material science. The simplest example is analysis of elastic fields due to inclusions in an infinite space, which has been considered in Section 3. Rodin (1996) has described an approach to find the Eshelby tensor in this case by subdividing the inclusion in rectangular simplexes. Explicit calculations have been carried out by Nozaki and Taya (2001), who have arrived at bulky equations. Our method leads to relations (11), (18) and (19), which have essentially simpler form. Another advantage of this method is that one does not need to triangulate the inclusion surface. This reduces the calculations and makes the integration procedure more transparent.

We have generalized results of Glas (1991, 2001) concerning hydrostatic inclusions in a half-space in three respects. First, we have derived explicit analytical formulas for arbitrary polyhedral inclusions. Second, we have considered inclusions in bi-materials. Third, we have taken into account anisotropy effects. In addition, we have removed existing inaccuracy in calculation of stresses inside the inclusion.

We have analyzed anisotropy effects following the approach presented in Appendix B. This approach is based on the reflectivity method by Kennett (1983) and it has several advantages compared to methods presented in the literature (Pan and Chou, 1979b; Yu et al., 1995). It is physically more transparent, since the answer is expressed in terms of reflection and transmission matrices, and it is also applicable to multi-layered media. In previous studies, elastic fields of quantum dots in multi-layered media have been determined implicitly, as solutions of a system of algebraic equations (Yang and Pan, 2003). Recursion relations (B.22), (B.23) together with Eqs. (B.25) and (B.26) provide an explicit solution to the problem.

We have reduced standard expressions for the non-hydrostatic Green tensor to form (30), which contains only harmonic and higher harmonic functions, and hence it can be integrated analytically. This gives a complete solution to the problem of uniform non-hydrostatic polyhedral inclusions in a half-space. As an illustration, we have solved the Mindlin and Cherruti problems for polygons.

In the case of inclusions with a non-uniform eigenstrain, one deals with the same type of integrals, which can be found explicitely. This opens the possibility to carry out analytically calculations of finite-element type. The derived equations, being applied to the Newtonian potential, give the gravitational field produced by bodies whose density varies as a fourth order polynomial. Solution of this type has not been presented in the literature.

The method developed has been applied to calculate piezoelectric fields around quantum dots in both isotropic and anisotropic (transversely isotropic) media. In previous calculations of piezoelectric fields by Pan (2002a,b), the corresponding Green functions have been found only in Fourier space, except for the case of a traction-free conductive surface (Pan, 2002a). We not only have derived these Green functions in the coordinate space, but also have integrated them analytically over the inclusion volume. Note, that a cubic inclusion in an isotropic material reproduces fields of quantum dots in GaAs $(0,0,1)$ and GaAs $(1,1,1)$ depending on the orientation of the cube, see Figs. 8 and 9. This suggests that effects related to the lattice geometry can be qualitatively modeled by choosing an appropriate inclusion shape.

Our results can be also used in cases, where a fully-analytical solution is not feasible. For example, Sharma with co-authors have proposed to describe nonlocal effects in quantum dots by the Yukawa potential, $\exp(-r/\lambda)/r$, where λ is some characteristic length, and have analyzed the dot shape effects by calculating three dimensional integrals (Sharma and Dasgupta, 2002; Zhang and Sharma, 2005). In Appendix A we have expressed integrals of arbitrary functions $f(r)$ over polyhedral volumes through line integrals, which allows to significantly simplify calculations.

We expect that our results will help to better understand physical properties of quantum dots and they will be also useful in traditional geophysical and elasto-mechanical applications.

Acknowledgements

I would like to thank Shell International Exploration and Production B. V. for permission to publish this paper. I am grateful to Stephen Bourne and Bob Smits for stimulating discussions.

Appendix A. Basic integrals

In this Appendix we calculate integrals, which are used all across the paper. The derivation procedure is similar to what has been done in gravimetry theory (Holstein, 2002). An essential difference is that we carry out the calculations in a more general form, without using particular properties of the Newtonian potential.

A.1. Problem statement and notations

We consider volume integrals of the type

$$\int\int\int \frac{\partial}{\partial x_1}\frac{\partial}{\partial x_2}\cdots\frac{\partial}{\partial x_m} r^q \mathrm{d}V. \tag{A.1}$$

Here, q is an integer number, x_j are coordinates, and the integration is carried out over the volume of a polyhedron. Integrals (A.1) can be formally treated as contractions of the tensor

$$\boldsymbol{T}_m^{(q)} = \int\int\int \underbrace{(\nabla\otimes\ldots\otimes\nabla)}_{m \text{ times}} r^q \mathrm{d}V \tag{A.2}$$

with a set of coordinate vectors $\vec{\boldsymbol{e}}_1, \ldots, \vec{\boldsymbol{e}}_m$, i.e. as $\boldsymbol{T}_m^{(q)}(\vec{\boldsymbol{e}}_1, \ldots, \vec{\boldsymbol{e}}_m)$. Using Green's theorem, one expresses volume integrals (A.2) through surface integrals,

$$\boldsymbol{T}_m^{(q)} = \sum_{\text{polygons}} \vec{\boldsymbol{n}}\otimes\boldsymbol{\Phi}_{m-1}^{(q)}, \tag{A.3}$$

where

$$\boldsymbol{\Phi}_m^{(q)} = \int\int_{\text{polygon}} \underbrace{(\nabla\otimes\ldots\otimes\nabla)}_{m \text{ times}} r^q \quad \mathrm{d}S, \tag{A.4}$$

and $\vec{\boldsymbol{n}}$ is the normal vector to the surface in the outer direction.

A.2. Integrals $\boldsymbol{\Phi}_0^{(q)}$

An arbitrary vector $\vec{\mathbf{X}}_s$, which is parallel to a flat surface, $\vec{\boldsymbol{n}}\cdot\vec{\mathbf{X}}_s = 0$, satisfies the identity $\vec{\boldsymbol{n}}\cdot\nabla\times(\vec{\boldsymbol{n}}\times\vec{\mathbf{X}}_s) = \nabla\cdot\vec{\mathbf{X}}_s$. Using the Stokes theorem to integrate this identity over a polyhedron we arrive at

$$\int\int_{\text{polygon}} \nabla\cdot\vec{\mathbf{X}}_s \mathrm{d}S = \oint (\vec{\boldsymbol{n}}\times\vec{\mathbf{X}}_s)\cdot\mathrm{d}\vec{\mathbf{l}} = \sum_{\text{edges}} \int \vec{\boldsymbol{b}}\cdot\vec{\mathbf{X}}_s \mathrm{d}\tau. \tag{A.5}$$

Here, $\mathrm{d}\vec{\mathbf{l}} = \vec{\boldsymbol{v}}\mathrm{d}\tau$ and $\vec{\boldsymbol{v}}$ is the unit vector along the polygon edge. Direction of $\vec{\boldsymbol{v}}$ is determined by the convention that the polygon boundary is oriented counter-clockwise when looking at the surface from outside the polyhedron.

We apply Eq. (A.5) to the vector $\vec{\mathbf{X}}_s = \vec{\boldsymbol{r}}_s f/r_s^2$, where f is an arbitrary function and $\vec{\boldsymbol{r}}_s = \vec{\boldsymbol{r}} - \vec{\boldsymbol{n}}(\vec{\boldsymbol{n}}\cdot\vec{\boldsymbol{r}})$ is the projection of the radius vector on the surface. This results in

$$\int\int_{\text{polygon}} \frac{\vec{\boldsymbol{r}}_s\cdot\nabla f}{r_s^2}\mathrm{d}S = \sum_{\text{edges}} r_b \int \frac{f - f(\vec{\boldsymbol{r}}_n)}{r_s^2}\mathrm{d}r_v. \tag{A.6}$$

We have taken into account that $\nabla\cdot(\vec{r}_s/r_s^2)=\nabla^2\ln r_s=2\pi\delta(\vec{r}_s)$, where $\delta(\vec{r}_s)$ is the delta function in two dimensions, and have added the term proportional to $f(\vec{r}_n)$ to represent this delta function.

Eq. (A.6) for $f(r)=r^{q+2}$ gives

$$(q+2)\mathbf{\Phi}_0^{(q)}=\sum_{\text{edges}}[r_bI_q+r_n(J_q-|r_n|^qJ_0)], \tag{A.7}$$

where we have introduced the notations

$$I_q=\int r^q\mathrm{d}r_v,\quad J_q=r_nr_b\int\frac{r^q\mathrm{d}r_v}{r_s^2}. \tag{A.8}$$

The integral J_0 is related to the apex angle θ as $J_0=r_n\theta$, the integral I_0 is found by elementary integration, $I_0=\int\mathrm{d}r_v=r_v$, and the integrals I_{-1} and J_{-1} are equal to

$$I_{-1}=\ln(r+r_v)|_{\tau_1}^{\tau_2},\quad J_{-1}=\arctan\left(\frac{r_nr_v}{r_br}\right)\Bigg|_{\tau_1}^{\tau_2}. \tag{A.9}$$

Using the recurrence relations

$$(1+q)I_q=r_vr^q+qr_\perp^2I_{q-2},\quad J_q=r_nr_bI_{q-2}+r_n^2J_{q-2}, \tag{A.10}$$

where $r_\perp=(r_b^2+r_n^2)^{1/2}$, one determines the integrals I_q and J_q for all q. Substituting Eq. (A.10) into Eq. (A.7) we obtain the recurrence relation for $\mathbf{\Phi}_0^{(q)}$,

$$(q+2)\mathbf{\Phi}_0^{(q)}=qr_n^2\mathbf{\Phi}_0^{(q-2)}+\sum_{\text{edges}}r_bI_q, \tag{A.11}$$

which involves computation of I_q only.

A.3. Integrals with derivatives of functions

Once the values $\mathbf{\Phi}_0^{(q)}$ are known, the integrals $\mathbf{\Phi}_m^{(q)}$ can be also calculated analytically. One can do it by making the substitution $\vec{r}\to\vec{r}-\vec{r}_0$ in expressions for $\mathbf{\Phi}_0^{(q)}$ and then differentiating them with respect to components of $\vec{r}_0$. Since such a procedure is very tedious (MacMillan, 1930), we use direct integration.

Decomposing the gradient of an arbitrary function f as $\nabla f=(\vec{n}\cdot\nabla f)\vec{n}+\nabla_s f$, where $\nabla_s f$ denotes differentiation in the polygon plane, and using Eq. (A.5) we obtain

$$\int\int_{\text{polygon}}\nabla f\mathrm{d}S=\sum_{\text{edges}}\vec{b}\int f\mathrm{d}\tau+\vec{n}\int\int_{\text{polygon}}(\vec{n}\cdot\nabla f)\mathrm{d}S. \tag{A.12}$$

For power functions $f(r)=r^q$, from Eqs. (A.6) and (A.12) it follows

$$\mathbf{\Phi}_1^{(q)}=\sum_{\text{edges}}[\vec{b}I_q+\vec{n}(J_q-|r_n|^qJ_0)], \tag{A.13}$$

which can be also written as the recurrence relation $\mathbf{\Phi}_1^{(q)}=qr_n\vec{n}\mathbf{\Phi}_0^{(q-2)}+\sum\vec{b}I_q$.

A.4. Higher order derivatives

Applying Eq. (A.12) to $f=\nabla F$, after some algebra we find

$$\int\int_{\text{polygon}}\nabla\otimes\nabla F\mathrm{d}S=\vec{n}\otimes\vec{n}\int\int_{\text{polygon}}\nabla^2F\mathrm{d}S+\sum_{\text{edges}}\left[\vec{b}\otimes\vec{v}F\Big|_{\tau_1}^{\tau_2}+(\vec{b}\otimes\vec{n}+\vec{n}\otimes\vec{b})\int\vec{n}\cdot\nabla F\mathrm{d}\tau\right.$$
$$\left.+(\vec{b}\otimes\vec{b}-\vec{n}\otimes\vec{n})\int\vec{b}\cdot\nabla F\mathrm{d}\tau\right]. \tag{A.14}$$

If the function F is harmonic, then the first term in the right side of Eq. (A.14) vanishes, so that the volume integral is expressed through line integrals. If $F=r^q$, then Eq. (A.14) reduces to

$$\mathbf{\Phi}_2^{(q)} \equiv \int\int_{\text{polygon}} \nabla \otimes \nabla r^q \mathrm{d}S = q(q+1)\vec{\boldsymbol{n}} \otimes \vec{\boldsymbol{n}} \mathbf{\Phi}_0^{(q-2)} + \sum_{\text{edges}} \left\{ \vec{\boldsymbol{b}} \otimes \vec{\boldsymbol{v}} r^q \big|_{\tau_1}^{\tau_2} + q\left[\left(\vec{\boldsymbol{b}} \otimes \vec{\boldsymbol{n}} + \vec{\boldsymbol{n}} \otimes \vec{\boldsymbol{b}} \right) r_n + \left(\vec{\boldsymbol{b}} \otimes \vec{\boldsymbol{b}} - \vec{\boldsymbol{n}} \otimes \vec{\boldsymbol{n}} \right) r_b \right] I_{q-2} \right\}. \tag{A.15}$$

Differentiation of Eq. (A.15) gives

$$\mathbf{\Phi}_3^{(q)} = q(q+1)\vec{\boldsymbol{n}} \otimes \vec{\boldsymbol{n}} \mathbf{\Phi}_1^{(q-2)} + q \sum_{\text{edges}} \left\{ \vec{\boldsymbol{b}} \otimes \vec{\boldsymbol{v}} \otimes \vec{\boldsymbol{r}} r^{q-2} \Big|_{\tau_1}^{\tau_2} + [(\vec{\boldsymbol{b}} \otimes \vec{\boldsymbol{n}} + \vec{\boldsymbol{n}} \otimes \vec{\boldsymbol{b}}) r_n + (\vec{\boldsymbol{b}} \otimes \vec{\boldsymbol{b}} - \vec{\boldsymbol{n}} \otimes \vec{\boldsymbol{n}}) r_b] \otimes \left[\vec{\boldsymbol{v}} r^{q-2} \big|_{\tau_1}^{\tau_2} + (q-2)\vec{\boldsymbol{r}}_\perp I_{q-4} \right] + [(\vec{\boldsymbol{b}} \otimes \vec{\boldsymbol{n}} + \vec{\boldsymbol{n}} \otimes \vec{\boldsymbol{b}}) \otimes \vec{\boldsymbol{n}} + (\vec{\boldsymbol{b}} \otimes \vec{\boldsymbol{b}} - \vec{\boldsymbol{n}} \otimes \vec{\boldsymbol{n}}) \otimes \vec{\boldsymbol{b}}] I_{q-2} \right\}, \tag{A.16}$$

where $\vec{\boldsymbol{r}}_\perp = r_n \vec{\boldsymbol{n}} + r_b \vec{\boldsymbol{b}}$.

To derive integrals with higher order derivatives one replaces F in Eq. (A.14) by $\nabla \otimes \ldots \nabla \otimes F$.

Appendix B. Transversely isotropic medium

Green's function problem for transversely isotropic half-spaces and bi-materials was investigated in numerous studies. The history of the problem and explicit expressions are presented by Pan and Chou (1979a,b); Walker, 1993; Yu et al. (1994, 1995); Yue, 1995; Yu and Rath, 2000. Liao and Wang (1998, 1999) review solutions for displacements, strains, and stresses in a half-space subjected to different types of loads. In this Appendix we outline an alternative derivation of Green's functions, which is based on the reflectivity method by Kennett (1974, 1983) (see also Fuchs and Müller (1971) and Müller (1985)). This is the standard method in theory of seismic waves in horizontally layered media (Booth and Crampin, 1983; Ursin, 1983; Fryer and Frazer, 1984), and it turns out to be an effective tool in geomechanical calculations (Kuvshinov, 2007b).

B.1. Governing equations

The momentum balance equation and the stress–strain relation describing a uniform elastic layer with arbitrary anisotropy can be reduced to a set of first order differential equations with respect to the vertical coordinate z (Woodhouse, 1974). For a transversely isotropic layer these equations have the form (Takeuchi and Saito, 1972; Kennett, 1983),

$$\frac{\partial}{\partial z} \nabla \cdot \vec{\boldsymbol{u}}_\perp = \frac{1}{N} \nabla \cdot \vec{\boldsymbol{\tau}}_{\perp z} - \nabla_\perp^2 u_z, \tag{B.1}$$

$$\frac{\partial u_z}{\partial z} = \frac{1}{H} (\tau_{zz} - F \nabla \cdot \vec{\boldsymbol{u}}_\perp), \tag{B.2}$$

$$\frac{\partial \tau_{zz}}{\partial z} = \rho \frac{\partial^2 u_z}{\partial t^2} - \nabla \cdot \vec{\boldsymbol{\tau}}_{\perp z} - F_z, \tag{B.3}$$

$$\frac{\partial}{\partial z} \nabla \cdot \vec{\boldsymbol{\tau}}_{\perp z} = \left[\rho \frac{\partial^2}{\partial t^2} - \left(B - \frac{F^2}{H} \right) \nabla_\perp^2 \right] \nabla \cdot \vec{\boldsymbol{u}}_\perp - \frac{F}{H} \nabla_\perp^2 \tau_{zz} - \nabla \cdot \vec{\boldsymbol{F}}_\perp, \tag{B.4}$$

$$\frac{\partial}{\partial z} (\nabla \times \vec{\boldsymbol{u}})_z = \frac{1}{N} (\nabla \times \vec{\boldsymbol{\tau}}_{\perp z})_z, \tag{B.5}$$

$$\frac{\partial}{\partial z} (\nabla \times \vec{\boldsymbol{\tau}}_{\perp z})_z = \left(\rho \frac{\partial^2}{\partial t^2} - G \nabla_\perp^2 \right) (\nabla \times \vec{\boldsymbol{u}}_\perp)_z - (\nabla \times \vec{\boldsymbol{F}}_\perp)_z. \tag{B.6}$$

Here, B, H, N, F, and G are elastic moduli of the medium, which are expressed through Voigt constants C_{jk} as

$$B = C_{11}, \quad H = C_{33}, \quad N = C_{44}, \quad F = C_{13}, \quad G = C_{66}, \tag{B.7}$$

and we have introduced the notation $\vec{\boldsymbol{\tau}}_{\perp z} = (\tau_{xz}, \tau_{yz}, 0)$. In the fully isotropic case $B = H$, $G = N$, and $F = H - 2N$. The peculiarity of a transversely isotropic medium is that six Eqs. (B.1)–(B.6) split in two independent groups. For this reason, closed form analytical expressions for Green's functions in such media can be

found. Four Eqs. (B.1)–(B.4) describe deformations with the vertical polarization. Two equations (B.5) and (B.6) describe deformations with the horizontal polarization.

We consider dilatational deformations caused by a potential external force $\vec{\mathbf{f}} = -\nabla p$. Since $\nabla \times \vec{\mathbf{f}} = 0$, the deformations with the horizontal polarization are absent. We apply an integral transform in the horizontal plane, which converts the Laplacian operator into a multiplicative operator

$$\nabla^2 \to k_\perp^2, \tag{B.8}$$

where $k_\perp$ has the meaning of a horizontal wave vector. Assuming a harmonic time dependence of the form $\exp(-\mathrm{i}\omega)$, we reduce equations for deformations with the vertical polarization to

$$\frac{\partial}{\partial \hat{z}} \underbrace{\begin{pmatrix} \nabla \cdot \hat{\vec{\boldsymbol{u}}}_\perp \\ \hat{\tau}_{zz} \\ \frac{\nabla \cdot \hat{\vec{\tau}}_{\perp z}}{k_\perp} \\ k_\perp \hat{u}_z \end{pmatrix}}_{\vec{\psi}} = \underbrace{\begin{pmatrix} 0 & 0 & 1/N & 1 \\ 0 & 0 & -1 & -\Omega^2 \\ -\Omega^2 + B - F^2/H & F/H & 0 & 0 \\ -F/H & 1/H & 0 & 0 \end{pmatrix}}_{\boldsymbol{A}} + \underbrace{\begin{pmatrix} 0 \\ 0 \\ \hat{p} \\ 0 \end{pmatrix}}_{\vec{\hat{f}}}. \tag{B.9}$$

Here, $\Omega^2 = \rho\omega^2/k_\perp^2$ is the normalized frequency, $k_\perp$ is the horizontal wave vector, $\hat{z} = k_\perp z$, and hats with other variables denote their integral transforms.

B.2. Eigenmodes and eigenvalues

The matrix $\boldsymbol{A}$ in Eq. (B.9) has four eigenvalues, $\pm\lambda_+$ and $\pm\lambda_-$, where $\mathrm{Re}(\lambda_\pm) > 0$. The squares of eigenvalues $\lambda_\pm^2$ are determined by the dispersion relation

$$\lambda_\pm^2 = \frac{1}{2}\left(b \pm \sqrt{b^2 - 4c}\right), \tag{B.10}$$

with

$$b = \frac{BH - F(F+2N) - (H+N)\Omega^2}{NH}, \quad c = \frac{(B-\Omega^2)(N-\Omega^2)}{NH}. \tag{B.11}$$

The eigenvectors of $\boldsymbol{A}$ are columns of the matrix $\boldsymbol{M}$,

$$\boldsymbol{M} = \begin{pmatrix} 1 & 1 & 1 & 1 \\ -s_- & -s_+ & -s_- & -s_+ \\ q_+ s_+ & q_- s_- & -q_+ s_+ & -q_- s_- \\ -q_+ & -q_- & q_+ & q_- \end{pmatrix} \tag{B.12}$$

The order of columns of $\boldsymbol{M}$ is specified according to the order of eigenvalues λ_+, λ_-, $-\lambda_+$, $-\lambda_-$. The constants $s_\pm$ and $q_\pm$ entering Eq. (B.12) are equal to

$$s_\pm = N\frac{H\lambda_\pm^2 + F + \Omega^2}{F+N}, \quad q_\pm = \frac{B - \Omega^2 - N\lambda_\pm^2}{\lambda_\pm(F+N)}. \tag{B.13}$$

Once the eigenvalues and eigenvectors of the matrix $\boldsymbol{A}$ are known, one obtains the general solution of Eq. (B.9),

$$\vec{\boldsymbol{\psi}}(z) = \boldsymbol{M} \cdot \vec{\boldsymbol{C}} + \vec{\boldsymbol{\psi}}_{\mathrm{part}}, \vec{\boldsymbol{C}}(z) = \mathrm{e}^{\boldsymbol{E}(\hat{z}-\hat{z}_0)} \cdot \vec{\boldsymbol{C}}(z_0). \tag{B.14}$$

Here, $\vec{\boldsymbol{\psi}}_{\mathrm{part}}$ is a particular solution of Eq. (B.9),

$$\vec{\boldsymbol{\psi}}_{\mathrm{part}} = \frac{\hat{p}}{B-\Omega^2}(1, \quad F, \quad 0, \quad 0)^{\mathrm{T}}, \tag{B.15}$$

$\boldsymbol{E}$ is the eigenvalue matrix, and

$$e^{\boldsymbol{E}(\hat{z}-\hat{z}_0)} = \begin{pmatrix} e^{\lambda_+(\hat{z}-\hat{z}_0)} & 0 & 0 & 0 \\ 0 & e^{\lambda_-(\hat{z}-\hat{z}_0)} & 0 & 0 \\ 0 & 0 & e^{-\lambda_+(\hat{z}-\hat{z}_0)} & 0 \\ 0 & 0 & 0 & e^{-\lambda_-(\hat{z}-\hat{z}_0)} \end{pmatrix}. \tag{B.16}$$

We have assumed that the matrix $\boldsymbol{A}$ is non-degenerate, so that its four eigenvalues are distinct. If the matrix $\boldsymbol{A}$ is degenerate, then the eigenvalue matrix $\boldsymbol{E}$ is replaced by the Jordan matrix, and one composes the matrix $\boldsymbol{M}$ from the generalized eigenvectors of $\boldsymbol{A}$ (Kuvshinov, 2007b).

B.3. Reflection and transmission matrices

Eq. (B.14) can be viewed as a translation rule for the vector $\vec{\boldsymbol{C}}$. In the absence of external forces $\vec{\boldsymbol{C}}(\beta) = \boldsymbol{Q}(\beta,\alpha)\cdot\vec{\boldsymbol{C}}(\alpha)$. If points α and β belong to the same material, then $\boldsymbol{Q}(\beta,\alpha) = \exp[\boldsymbol{E}(\hat{z}_\beta - \hat{z}_\alpha)]$, where $\hat{z}_\alpha$ and $\hat{z}_\beta$ are normalized vertical coordinates of corresponding points. If points "α" and "β" belong to different materials separated by a horizontal interface, then from the condition $\vec{\boldsymbol{\psi}}(\alpha) = \vec{\boldsymbol{\psi}}(\beta)$ it follows

$$\boldsymbol{Q}(\beta,\alpha) = \boldsymbol{M}^{-1}(\beta)\cdot\boldsymbol{M}(\alpha). \tag{B.17}$$

Direct calculation shows that the matrix $\boldsymbol{Q}$ in Eq. (B.17) has a symmetric block structure,

$$\boldsymbol{Q}(\beta,\alpha) = \begin{pmatrix} \boldsymbol{Q}_u(\beta,\alpha) & \boldsymbol{Q}_d(\beta,\alpha) \\ \boldsymbol{Q}_d(\beta,\alpha) & \boldsymbol{Q}_u(\beta,\alpha) \end{pmatrix}, \tag{B.18}$$

with

$$\boldsymbol{Q}_{u,d}(\beta,\alpha) = \frac{1}{2[s_+(\beta)-s_-(\beta)]}\begin{pmatrix} -\Delta^{(-,+)} \pm \frac{q_+(\alpha)}{q_+(\beta)}\Delta^{(+,-)} & -\Delta^{(+,+)} \pm \frac{q_-(\alpha)}{q_+(\beta)}\Delta^{(-,-)} \\ \Delta^{(-,-)} \mp \frac{q_+(\alpha)}{q_-(\beta)}\Delta^{(+,+)} & \Delta^{(+,-)} \mp \frac{q_-(\alpha)}{q_-(\beta)}\Delta^{(-,+)} \end{pmatrix}. \tag{B.19}$$

Here, $\Delta^{(\sigma_1,\sigma_2)} = s_{\sigma_1}(\alpha) - s_{\sigma_2}(\beta)$, the upper sign in "$\pm$" and "$\mp$" refers to $\boldsymbol{Q}_u$ and the lower sign refers to $\boldsymbol{Q}_d$.

The vector $\vec{\boldsymbol{C}}$ has four components. The sub-vector $\vec{\boldsymbol{C}}_u$ composed from the first two components of $\vec{\boldsymbol{C}}$ describes amplitudes of the eigenmodes propagating in the negative direction (opposite to $\vec{\boldsymbol{e}}_z$). The complimentary sub-vector $\vec{\boldsymbol{C}}_d$ describes amplitudes of the eigenmodes propagating along $\vec{\boldsymbol{e}}_z$. Kuvshinov (2007b) has shown that LU-decomposition of the matrix $\boldsymbol{Q}$ gives the reflection and transmission matrices for vectors $\vec{\boldsymbol{C}}_{u,d}$, which in accordance with the reflectivity method of Kennett (1983) are equal to

$$\boldsymbol{T}(\alpha,\beta) = \boldsymbol{Q}_u(\beta,\alpha)^{-1}, \quad \boldsymbol{R}(\beta,\alpha) = -\boldsymbol{T}(\alpha,\beta)\cdot\boldsymbol{Q}_d(\beta,\alpha). \tag{B.20}$$

Since Eq. (B.20) contains only 2×2 matrices, the calculation of $\boldsymbol{T}$ and $\boldsymbol{R}$ is straightforward, although it leads to bulky expressions. If the medium "β" is infinitely soft, then the elements of the reflection matrix $\boldsymbol{R}(\beta,\alpha)$ are equal to

$$R_{11} = -R_{22} = \frac{q_+ s_+^2 + q_- s_-^2}{q_+ s_+^2 - q_- s_-^2}, \quad R_{12} = \frac{2q_- s_+ s_-}{q_+ s_+^2 - q_- s_-^2}, \quad R_{21} = -\frac{2q_+ s_+ s_-}{q_+ s_+^2 - q_- s_-^2}. \tag{B.21}$$

Eq. (B.20) determines transmission and reflection matrices through interfaces. The reflection matrix through a uniform layer vanishes. The transmission matrix through a uniform layer is equal to $\exp[-\boldsymbol{E}_+(\hat{z}_\beta - \hat{z}_\alpha)]$ for $\hat{z}_\beta > \hat{z}_\alpha$ and to $\exp[\boldsymbol{E}_+(\hat{z}_\beta - \hat{z}_\alpha)]$ for $\hat{z}_\beta < \hat{z}_\alpha$. Here, $\boldsymbol{E}_+$ is the upper-left 2×2 sub-block of the eigenvalue matrix $\boldsymbol{E}$.

B.4. Matching procedure

Let's consider a medium consisting of uniform, horizontal layers. The external "pressure" p is applied to the plane $z = z_s$. We treat this plane as a layer with an infinitely small thickness h_s and call it the "source layer". The vertical derivative of p vanishes inside the "source layer", $\partial p/\partial z = 0$, while its horizontal

derivatives there can be arbitrary. Starting from the outmost interfaces and using the composition rules for the reflection and transmission matrices (Kennett, 1983)

$$\boldsymbol{T}(a,c) = \boldsymbol{T}(a,b)\cdot[\mathbf{I}-\boldsymbol{R}(c,b)\cdot\boldsymbol{R}(a,b)]^{-1}\cdot\boldsymbol{T}(b,c), \tag{B.22}$$

$$\boldsymbol{R}(a,c) = \boldsymbol{R}(b,c)+\boldsymbol{T}(c,b)\cdot\boldsymbol{R}(a,b)\cdot[\mathbf{I}-\boldsymbol{R}(c,b)\cdot\boldsymbol{R}(a,b)]^{-1}\cdot\boldsymbol{T}(b,c), \tag{B.23}$$

one determines the reflection matrices $\boldsymbol{R}_+ \equiv \boldsymbol{R}(\infty,z_+)$ and $\boldsymbol{R}_- \equiv \boldsymbol{R}(-\infty,z_-)$. Here, $z_\pm$ are points lying just outside the "source layer" in the positive and negative vertical direction correspondingly. The sub-vectors $\vec{\boldsymbol{C}}_u$ and $\vec{\boldsymbol{C}}_d$ at points $z_\pm$ are related as

$$\vec{\boldsymbol{C}}_d(z_-) = \boldsymbol{R}_-\cdot\vec{\boldsymbol{C}}_u(z_-), \qquad \vec{\boldsymbol{C}}_u(z_+) = \boldsymbol{R}_+\cdot\vec{\boldsymbol{C}}_d(z_+). \tag{B.24}$$

Taking into account that the value $\tau_{zz}-p$ is continuous and matching solution (B.14) across the "source layer" one has

$$(\mathbf{I}-\boldsymbol{R}_+\cdot\boldsymbol{R}_-)\cdot\vec{\boldsymbol{C}}_u(z_-) = C_0(\mathbf{I}+\boldsymbol{R}_+)\cdot\begin{pmatrix}\lambda_+a_+\\ \lambda_-a_-\end{pmatrix}, \tag{B.25}$$

$$(\mathbf{I}-\boldsymbol{R}_-\cdot\boldsymbol{R}_+)\cdot\vec{\boldsymbol{C}}_d(z_+) = C_0(\mathbf{I}+\boldsymbol{R}_-)\cdot\begin{pmatrix}\lambda_+a_+\\ \lambda_-a_-\end{pmatrix}. \tag{B.26}$$

Here,

$$C_0 = \frac{k_\perp h_s\hat{p}}{B-\Omega^2}, \quad a_+ = \frac{s_++F-B}{2(s_+-s_-)}, \quad a_- = -\frac{s_-+F-B}{2(s_+-s_-)}. \tag{B.27}$$

Eqs. (B.22)–(B.26) provide a complete description of hydrostatic deformations of a multi-layered medium. We apply these equations for the case of bi-materials. The components of the vector $\vec{\boldsymbol{\psi}}$ in the material to which the force is applied are equal to

$$\nabla\cdot\hat{\vec{\boldsymbol{u}}}^G_\perp = C_0[a_1\mathrm{e}^{-\lambda_+|\hat{d}-\hat{z}|}+a_2\mathrm{e}^{-\lambda_-|\hat{d}-\hat{z}|}+a_{31}e^{-\lambda_+(\hat{d}+\hat{z})}+a_{32}e^{-(\lambda_-\hat{d}+\lambda_+\hat{z})}+a_{41}e^{-(\lambda_+\hat{d}+\lambda_-\hat{z})}+a_{42}e^{-\lambda_-(\hat{d}+\hat{z})}], \tag{B.28}$$

$$\hat{\tau}^G_{zz} = -C_0\{s_-a_1e^{-\lambda_+|\hat{d}-\hat{z}|}+s_+a_2\mathrm{e}^{-\lambda_-|\hat{d}-\hat{z}|}+s_-[a_{31}\mathrm{e}^{-\lambda_+(\hat{d}+\hat{z})}+a_{32}\mathrm{e}^{-(\lambda_-\hat{d}+\lambda_+\hat{z})}]+s_+[a_{41}\mathrm{e}^{-(\lambda_+\hat{d}+\lambda_-\hat{z})}+a_{42}\mathrm{e}^{-\lambda_-(\hat{d}+\hat{z})}]\}, \tag{B.29}$$

$$\frac{\nabla\cdot\hat{\vec{\boldsymbol{\tau}}}^G_{\perp z}}{k_\perp} = C_0\{q_+s_+a_1\mathrm{e}^{-\lambda_+|\hat{d}-\hat{z}|}+q_-s_-a_2\mathrm{e}^{-\lambda_-|\hat{d}-\hat{z}|}-q_+s_+[a_{31}\mathrm{e}^{-\lambda_+(\hat{d}+\hat{z})}+a_{32}\mathrm{e}^{-(\lambda_-\hat{d}+\lambda_+\hat{z})}] - q_-s_-[a_{41}\mathrm{e}^{-(\lambda_+\hat{d}+\lambda_-\hat{z})}+a_{42}\mathrm{e}^{-\lambda_-(\hat{d}+\hat{z})}]\}, \tag{B.30}$$

$$k_\perp\hat{u}^G_z = C_0\{-q_+a_1\mathrm{e}^{-\lambda_+|\hat{d}-\hat{z}|}-q_-a_2\mathrm{e}^{-\lambda_-|\hat{d}-\hat{z}|}+q_+[a_{31}\mathrm{e}^{-\lambda_+(\hat{d}+\hat{z})}+a_{32}\mathrm{e}^{-(\lambda_-\hat{d}+\lambda_+\hat{z})}]+q_-[a_{41}\mathrm{e}^{-(\lambda_+\hat{d}+\lambda_-\hat{z})}+a_{42}\mathrm{e}^{-\lambda_-(\hat{d}+\hat{z})}]\}. \tag{B.31}$$

Here,

$$a_{i1} = a_+R_{i1}, \quad a_{i2} = a_-R_{i2}, \tag{B.32}$$

R_{ij} are elements of the reflection matrix $\boldsymbol{R}(\beta,\alpha)$, where "$\alpha$" labels the medium containing the inclusion and "β" labels the other medium. All the other parameters in Eqs. (B.28)–(B.31) refer to the medium "α".

The exact form of the integral transform (B.8) has not been specified yet. It is convenient to apply the zero order Hankel transform to calculate Green's functions for a dilatational source. In this case $\hat{p} = 1/(2\pi)$. Taking $\Omega = 0$ and using the relation

$$\int_0^\infty k_\perp^n J_0(k_\perp\rho)\mathrm{e}^{-k_\perp z}\mathrm{d}k_\perp = \frac{\partial^n}{\partial z^n}\frac{(-1)^n}{(\rho^2+z^2)^{1/2}} \tag{B.33}$$

to perform the inverse Hankel transform, one arrives at Eqs. (27) and (28).

Appendix C. Non-symmetric harmonic potential

Green's tensor representing elastic deformations induced by inclusions with non-hydrostatic strains contains the function $\chi = \vec{a}\cdot\vec{r}\ln(r+\vec{a}\cdot\vec{r}) - r$, where $\vec{a}$ is a constant unit vector. In contrast to the potentials considered in Appendix A, it is not spherically symmetric. However, the potential χ is harmonic, $\nabla^2\chi = 0$, which allows to reduce volume integrals to line integrals using Eqs. (A.3) and (A.14).

C.1. Inclusions

To find elastic deformations induced by strain inclusions, one needs to calculate integrals of the type

$$\int\int\int \nabla\otimes\nabla\otimes\nabla\chi\,\mathrm{d}V = \vec{n}\otimes\sum_{\text{polygons}}\sum_{\text{edges}}\left[\vec{b}\otimes\vec{v}\chi\Big|_{\tau_1}^{\tau_2} + \left(\vec{b}\otimes\vec{n}+\vec{n}\otimes\vec{b}\right)\int\vec{n}\cdot\nabla\chi\,\mathrm{d}\tau + (\vec{b}\otimes\vec{b}-\vec{n}\otimes\vec{n})\int\vec{b}\cdot\nabla\chi\,\mathrm{d}\tau\right]. \tag{C.1}$$

Line integrals in Eq. (C.1) are given by the expressions,

$$\int\nabla_\perp\chi\,\mathrm{d}\tau = \vec{a}_\perp[r_v\ln(r+\vec{a}\cdot\vec{r}) + r_\perp^2 L_{-1} + \vec{a}_\perp\cdot\vec{r}_\perp L_0 - L_1] - \vec{r}_\perp L_0, \tag{C.2}$$

$$L_n = L_n(\vec{a}) = \int\frac{r^n\mathrm{d}r_v}{r+\vec{a}\cdot\vec{r}}, \tag{C.3}$$

where the subscript "$\perp$" indicates direction perpendicular to the integration path, e.g. $\vec{r}_\perp = \vec{r} - r_v\vec{v}$. The integrals $\int\vec{n}\cdot\nabla\chi\,\mathrm{d}\tau$ and $\int\vec{b}\cdot\nabla\chi\,\mathrm{d}\tau$ are obtained if one multiplies the right side of Eq. (C.2) on $\vec{n}$ and $\vec{b}$ correspondingly.

If the vector $\vec{a}$ is parallel to $\vec{v}$ then

$$L_n = \int\frac{r^n\mathrm{d}r_v}{r\pm r_v} = \frac{1}{r_\perp^2}\left(I_{n+1}\mp\frac{r^{n+2}}{n+2}\right). \tag{C.4}$$

If the vector $\vec{a}$ lays parallel to $\vec{r}_\perp$ (recall that $\vec{r}_\perp$ is constant along the integration path) then

$$L_n = \int\frac{r^n\mathrm{d}r_v}{r\pm r_\perp} = (n+1)\left(I_{n-1}\mp\frac{I_n}{r_\perp}\right) - \frac{r^n}{r_v r_\perp}(r\mp r_\perp). \tag{C.5}$$

To find integrals L_n for the case $|a_v| = |\vec{a}\cdot\vec{v}| \neq 1$ and $\beta = |\vec{a}_\perp\cdot\vec{r}_\perp|/r_\perp \neq 1$, one introduces the "angle" variable $\gamma = \arctan(r_v/r_\perp)$, and makes the substitution $u = \tan(\gamma/2)$. In terms of the variable u the integrals L_n reduce to

$$L_n = 2r_\perp^n\int\left(\frac{1+u^2}{1-u^2}\right)^{n+1}\frac{\mathrm{d}u}{(\ldots)}, \tag{C.6}$$

where $(\ldots)$ is the quadratic polynomial of u,

$$(\ldots) = (1-\beta)u^2 + 2a_v u + 1 + \beta. \tag{C.7}$$

For $n = -1$,

$$\begin{aligned}\int\frac{\mathrm{d}u}{(\ldots)} &= \frac{1}{s^{1/2}}\arctan\frac{(1-\beta)u+a_v}{s^{1/2}}, && \beta^2+a_v^2\neq 1;\\ &= -[(1-\beta)u+a_v]^{-1}, && \beta^2+a_v^2 = 1;\end{aligned} \tag{C.8}$$

where $s = 1-\beta^2-a_v^2 \geqslant 0$. The integrals with $n \neq -1$ can be obtained recursively, using the standard technique of partial fraction decomposition.

The volume integrals containing forth order derivatives of the potential χ are given by Eq. (C.1), where one makes the formal substitution $\chi\to\nabla\chi$. In this case the line integrals in the right side of Eq. (C.1) contain values

$$\nabla\otimes\nabla\chi=\frac{\vec{a}\otimes\vec{a}-\sum_i\vec{e}_i\otimes\vec{e}_i}{r+\vec{a}\cdot\vec{r}}+\frac{r}{(r+\vec{a}\cdot\vec{r})^2}\left(\vec{a}+\frac{\vec{r}}{r}\right)\otimes\left(\vec{a}+\frac{\vec{r}}{r}\right),\tag{C.9}$$

where $\vec{e}_i$ are basis vectors of the coordinate system. It is sufficient to consider the case, where both operators ∇ in Eq. (C.9) act transversely to the vector $\vec{v}$. Then

$$\int\nabla_\perp\otimes\nabla_\perp\chi\mathrm{d}\tau=\left(\vec{a}_\perp\otimes\vec{a}_\perp-\sum_i\vec{e}_{i_\perp}\otimes\vec{e}_{i_\perp}\right)L_0+\vec{a}_\perp\otimes\vec{a}_\perp L_1^{(2)}+(\vec{a}_\perp\otimes\vec{r}_\perp+\vec{r}_\perp\otimes\vec{a}_\perp)L_0^{(2)}+\vec{r}_\perp\otimes\vec{r}_\perp L_{-1}^{(2)},\tag{C.10}$$

where the values $L_n^{(2)}$ are introduced as

$$L_n^{(2)}=\int\frac{r^n\mathrm{d}r_v}{(r+\vec{a}\cdot\vec{r})^2}=2r_\perp^{n-1}\int\left(\frac{1+u^2}{1-u^2}\right)^{n+1}\frac{(1-u^2)\mathrm{d}u}{(\dots)^2}.\tag{C.11}$$

Integrals $L_n^{(2)}$ are found essentially in the same way as integrals L_n.

C.2. Applied forces

In calculating elastic deformations due to applied forces one meets volume integrals containing second derivatives of χ, which reduce to Eq. (A.12). The line integrals in this equation are equal to

$$\begin{aligned}\int\chi\mathrm{d}\tau=&\left(\vec{a}_\perp\cdot\vec{r}_\perp+\frac{a_v r_v}{2}\right)r_v\ln(r+\vec{a}\cdot\vec{r})-r_v\vec{a}_\perp\cdot\vec{r}_\perp+\frac{r_\perp^2 I_{-1}}{2}-\frac{3I_1}{2}-\frac{1-a_v^2}{2}\left(r_\perp^2L_0-L_2\right)\\&+\frac{\vec{a}_\perp\cdot\vec{r}_\perp}{2}\left(r_\perp^2L_{-1}+2\vec{a}_\perp\cdot\vec{r}_\perp L_0+L_1\right).\end{aligned}\tag{C.12}$$

Since $\nabla^2\chi=0$, the gradient of χ is equal to the curl of some vector $\vec{\mathbf{X}}$, i.e. $\nabla\chi=\nabla\times\vec{\mathbf{X}}$. It can be checked that

$$\vec{\mathbf{X}}=(\vec{a}\times\vec{r})\left[\frac{1}{2}\ln(r+\vec{a}\cdot\vec{r})-\frac{r-\vec{a}\cdot\vec{r}}{4(r+\vec{a}\cdot\vec{r})}\right],\tag{C.13}$$

so that $\int\int\vec{n}\cdot\nabla\chi\mathrm{d}S=\int\int(\nabla\times\vec{\mathbf{X}})\cdot\mathrm{d}\vec{S}=\oint\vec{\mathbf{X}}\cdot\mathrm{d}\vec{\mathbf{l}}$. Line integrals are calculated analytically,

$$\int\int(\vec{n}\cdot\nabla\chi)\mathrm{d}S=\sum_{\text{edges}}\frac{\vec{v}\cdot(\vec{a}\times\vec{r})}{2}\times\left[r_v\ln(r+\vec{a}\cdot\vec{r})-\frac{r_v}{2}+r_\perp^2L_{-1}+\vec{a}_\perp\cdot\vec{r}_\perp L_0-L_1\right].\tag{C.14}$$

References

Andreev, A.D., O'Reilly, E.P., 2000. Theory of electronic structure of GaN/AlN hexagonal quantum dots. Phys. Rev. B 62, 15851–15870.

Andreev, A.D., Downes, J.R., Faux, D.A., O'Reilly, E.P., 1999. Strain distribution in quantum dots of arbitrary shape. J. Appl. Phys. 86, 297–305.

Benabbas, T., Androussi, P.F.Y., Lefebre, A., 1996. Stress relaxation in highly strained InAs/GaAs structures as studied by finite element analysis and transmission electron microscopy. J. Appl. Phys. 80, 2763–2767.

Beom, H.G., Kim, I.B., 1999. Analysis of a multilayered plate containing a cuboidal inclusion with eigenstrains. Mech. Mater. 31, 729–741.

Bimberg, D., Grundmann, M., Ledentsov, N.N., 1998. Quantum Dot Heterostructures. Wiley, New York.

Booth, D.C., Crampin, S., 1983. The anisotropic reflectivity technique: theory. Geophys. J. Roy. Astr. Soc. 72, 755–766.

Boussinesq, J., 1885. Applications des Potentiels à l'étude de l'équilibre et du mouvement des solids élastiques. Gauthier-Villars, Paris.

Cerutti, V., 1882. Ricerche intorno all'equilibrio dei elastici isotropi. Memorie della R. Accademia dei Lincei, Roma 13, 81–123.

Chinnery, M.A., 1961. The deformation of the ground around surface faults. Bull. Seism. Soc. Am. 50, 355–372.

Chinnery, M.A., 1963. The stress changes that accompany strike-slip faulting, Bull. Seism. Soc. Am. 53, 921–932.

Chiu, Y.P., 1977. On the stress field due to initial strains in a cuboid surrounded by an infinite elastic space. J. Appl. Mech. 44, 587–590.

Chiu, Y.P., 1978. On the stress field and surface deformation in a half space with a cuboidal zone in which initial strains are uniform. J. Appl. Mech. 45, 302–306.

Chowdhury, K.L.P., 1987. On the axisymmetric Mindlin's problem for a semi-space of granular material. Acta Mechanica 66, 145–160.

Chu, H.J., Wang, J., 2005. Strain distribution in arbitrarily shaped quantum dots with nonuniform composition. J. Appl. Phys. 98, 0343151–0343157.
Comninou, M., Dundurs, J., 1975. The angular dislocation in a half space. J. Elasticity 5, 203–216.
Cui, Y., Lieber, C.M., 2001. Functional nanoscale electronic devices assembled using silicon nanowires building blocks. Science 291, 851–853.
Cusack, M.A., Briddon, P.R., Jaros, M., 1997. Electronic structure of InAs/GaAs self-assembled quantum dots. Phys. Rev. B 54, R2300–R2303.
Daruka, I., Barabasi, A.L., Zhou, S.J., Germann, T.C., Lomdahl, P.S., Bishop, A.R., 1999. Molecular dynamics investigation of the surface stress distribution in a Ge/Si quantum dot superlattice. Phys. Rev. B 60, R2150–R2153.
Davies, J.H., Petticrew, D.E., Long, A.R., 1998. Theory of potential modulation in lateral surface superlattices. III. Two-dimensional superlatices and arbitrary surfaces. Phys. Rev. B 58, 10789–10799.
Davies, J.H., 1998. Elastic and piezoelectric fields around a buried quantum dot: a simple picture. J. Appl. Phys. 84, 1358–1365.
Davies, J.H., 1999. Quantum dots induced by strain from buried and surface stressors. Appl. Phys. Lett. 75, 4142–4144.
Davies, J.H., 2003. Elastic field in a semi-infinite solid due to thermal expansion or a coherently misfitting inclusion. J. Appl. Mech. 70, 655–660.
Downes, J.R., Faux, D.A., 1997. The Fourier-series method for calculating strain distributions in two dimensions. J. Phys.: Condens. Matter 9, 4509–4520.
Downes, J.R., Faux, D.A., O'Reilly, E.P., 1995. Influence of strain relaxation on the electronic properties of buried quantum wells and wires. Mater. Sci. Eng. B 35, 357–363.
Downes, J.R., Faux, D.A., O'Reilly, E.P., 1997. A simple method for calculating strain distributions in quantum dot structures. J. Appl. Phys. 81, 6700–6702.
Duan, H.L., Wang, J., Huang, Z.P., Karihaloo, B.L., 2005. Eshelby formalism for nano-inhomogeneities. Proc. R. Soc. Lond. A 461, 3335–3353.
Eshelby, J.D., 1957. The determination of the elastic field of an ellipsoidal inclusion, and related problems. Proc. R. Soc. Lond. A 252, 561–569.
Faivre, G., 1964. Déformations de cohérence dún précipite quadratique. Physica Stat. Sol. 35, 249–259.
Faux, D., Christmas, U.M.E., 2005. Real-space Green's tensors for stress and strain in crystals with cubic anisotropy. J. Appl. Phys. 98, 033534–033543.
Faux, D.A., Pearson, G.S., 2000. Green's tensors for anisotropic elasticity: applications to quantum dots. Phys. Rev. B 62, R4798–R4801.
Faux, D.A., Downes, J.R., O'Reilly, E.P., 1996. A simple method for calculating strain distributions in quantum wire structures. J. Appl. Phys. 84, 2515–2517.
Faux, D.A., Downes, J.R., O'Reilly, E.P., 1997. Analytic solutions for strain distributions in quantum wire structures. J. Appl. Phys. 82, 3754–3762.
Fryer, G.J., Frazer, L.N., 1984. Seismic waves in stratified anisotropic media. Geophys. J. Roy. Astr. Soc. 78, 691–710.
Fuchs, K., Müller, G., 1971. Computation of synthetic seismograms with the reflectivity method and comparison with observations. Geophys. J.R. Astron. Soc. 23, 417–433.
Gallardo-Delgado, L.A., Pérez-Flores, M.A., Gómez-Treviño, E., 2003. A versatile algorithm for joint 3D inversion of gravity and magnetic data. Geophysics 68, 949–959.
García-Abdeslem, J., 2005. The gravitational attraction of a right rectangular prism with density varying with depth following a cubic polynomial. Geophysics 70, J39–J42.
Geertsma, J.A., 1957. A remark on the analogy between thermoelasticity and the elasticity of saturated elastic porous media. J. Mech. Phys. Sol. 6, 13–16.
Geertsma, J., 1973. Land subsidence above compacting oil and gas reservoir. J. Petrol. Technol. 25, 734–744.
Glas, F., 1991. Coherent stress relaxation in a half space: modulated layers, inclusions, steps, and a general solution. J. Appl. Phys. 70, 3556–3571.
Glas, F., 2001. Elastic relaxation of truncated pyramidal quantum dots and quantum wires in a half-space: An analytical calculation. J. Appl. Phys. 90, 3232–3241.
Glas, F., 2002a. Analytical calculation of the strain field of single and periodic misfitting polygonal wires in half-space. Phil. Mag. A 82, 2591–2608.
Glas, F., 2002b. Elastic relaxation of isolated and interacting pyramidal quantum dots and quantum wires in a half space. Appl. Surf. Sci. 188, 9–18.
Glas, F., 2003. Elastic relaxation of a truncated circular cylinder with uniform dilatational eigenstrain in a half space. Phys. Status Solidi B 237, 599–610.
Goodier, J.N., 1937. On the integration of the thermoelastic equations. Phil. Mag. 7, 1017–1032.
Gossling, T.J., Willis, J.R., 1995. Mechanical stability and electronic properties of buried strained quantum wells arrays. J. Appl. Phys. 77, 5601–5610.
Götze, H.J., Lahmeyer, B., 1988. Application of three-dimensional interactive modeling in gravity and magnetics. Geophysics 53, 1096–1108.
Grundmann, M., Stier, O., Bimberg, D., 1995. InAs/GaAs pyramidal quantum dots: Strain distribution, optical phonons, and electronic structure. Phys. Rev. B 52, 11969–11981.
Gutkin, M.Y., Ovid'ko, I.A., Sheinerman, A.G., 2003. Misfit dislocations in composites with nanowires. J. Phys.: Condens. Matter. 15, 3539–3553.

Gutkin, M.Y., 2006. Elastic behavior of defects in nanomaterials I. Models for infinite and semi-infinite media. Rev. Adv. Mater. Sci. 13, 121–161.
Hansen, R.O., 1999. An analytical expression for the gravity field of a polyhedral body with linearly varying density. Geophysics 64, 75–77.
Harrison, P., 1999. Quantum Wells, Wires and Dots: Theoretical and Computational Physics. Wiley, New York.
Holstein, H., Ketteridge, B., 1996. Gravimetric analysis of uniform polyhedra. Geophysics 61, 357–364.
Holstein, H., Schürholz, P., Starr, A.J., Chakraborty, M., 1999. Comparison of gravimetric formulas for uniform polyhedra. Geophysics 64, 1438–1446.
Holstein, H., 2002. Gravimetric similarity in anomaly formulas for uniform polyhedra. Geophysics 67, 1126–1132.
Holstein, H., 2003. Gravimagnetic anomaly formulas for polyhedra of spatially linear media. Geophysics 68, 157–167.
Hu, S.M., 1989. Stress from a Parallelepipedic Thermal Inclusion in a Semispace. J. Appl. Phys. 66, 2741–2743.
Ignaczak, J., Nowacki, W., 1958. Two cases of discontinous fields in an elastic space and semi-space. Bull. Acad. Polon. Sci. Ser. Sci. Techn. 6, 309.
Jiang, X., Pan, E., 2004. Exact solution for 2D polygonal inclusion problem in anisotropic magnetoelectroelastic full-, half-, and bimaterial-planes. Int. J. Solids Struct. 41, 4361–4382.
Jogai, B., 2000. Three-dimensional strain field calculations in coupled InAs/GaAs quantum dots. J. Appl. Phys. 88, 5050–5055.
Jogai, B., 2001. Three-dimensional strain field calculations in multiple InN/AlN wurtzite quantum dots. J. Appl. Phys. 90, 699–704.
Johnson, H.T., Freund, L.B., 2001. The influence of strain on confined electronic states in semiconductor quantum structures. Int. J. Solids Struct. 94, 1045–1062.
Jonsdottir, F., Halldorsson, D., Beltz, G.E., Romanov, A.E., 2006. Buried stressors in nitride semiconductors: Influence on electronic properties. Model. Simul. Mater. Sci. Eng. 14, 1167–1180.
Kawashita, M., Nozaki, H., 2001. Eshelby tensor of a polygonal inclusion and its special properties. J. Elasticity 64, 71–84.
Kennett, B.L.N., 1974. Reflections, rays, and reverberations. Bull. Seism. Soc. Am. 64, 1685–1696.
Kennett, B.L.N., 1983. Seismic Wave Propagation in Stratified Media. Cambridge University Press, Cambridge.
Kikuchi, Y., Sugii, H., Shintani, K., 2001. Strain profiles in pyramidal quantum dots by means of atomistic calculations. J. Appl. Phys. 89, 1191–1196.
Kohler, C., 2003. Atomistic simulations of strain distributions in quantum dot nanostructures. J. Phys.: Condens. Matter 15, 133–146.
Kuvshinov, B.N., 2007a. Analytical geomechanical models. Offshore Magazine 67, 140–142.
Kuvshinov, B.N., 2007b. Reflectivity method for geomechanical equilibria. Geophys. J. Int. 170, 567–579.
Larkin, I.A., Davies, J.H., Long, A.R., Cuscó, R., 1997. Theory of potential modulation in lateral surface superlatices. II. Piezoelectric interaction. Phys. Rev. B 56, 15242–15251.
Li, Q., Anderson, P.M., 2001. A compact solution for the stress field from a cuboidal region with a uniform transformation strain. J. Elasticity 64, 237–245.
Li, X., Chouteau, M., 1998. Three dimensional gravity modeling in all space. Surveys Geophys. 19, 339–368.
Liao, J.J., Wang, C.D., 1998. Elastic solutions for a transversely isotropic half-space subjected to a point load. Int. J. Numer. Anal. Meth. Geomech. 22, 425–447.
MacMillan, W.D., 1930. Theory of the Potential. Dover Publications, New York.
Maerten, F., Resor, P., Pollard, D., Maerten, L., 2005. Inverting for slip on three-dimensional fault surfaces using angular dislocations. Bull. Seism. Soc. Am. 95, 1654–1665.
Makeev, M.A., Madhukar, A., 2001. Simulations of atomic level stresses in systems of buried Ge/Si islands. Phys. Rev. Lett. 86, 5542–5545.
Maranganti, R., and Sharma, P., 2005. A review of strain field calculations in embedded quantum dots and wires, In: Rieth, M. and Schommers, W. (Eds.), Handbook of Theoretical and Computational Nanotechnology (Chapter 118).
Mi, C., Kouris, D., 2006. Nanoparticle under the influence of surface/interface elasticity. J. Mech. Mater. Struct. 1, 763–791.
Mindlin, R.D., Cheng, D.H., 1950. Thermoelastic stress in the semi-infinite solid. J. Appl. Phys. 21, 931–933.
Mindlin, R.D., 1936. Force at a point in the interior of a semi-infinite solid. Physics 7, 195–202.
Moschovidis, Z.A., Mura, T., 1975. Two ellipsoidal inhomogeneities by the equivalent inclusion method. J. Appl. Mech. 42, 847–852.
Müller, G., 1985. The reflectivity method: a tutorial. J. Geophys. 58, 153–174.
Mura, T., 1987. Micromechanics of Defects in Solids. Martinus Nijhoff Publishers, Dordrecht.
Nowacki, W., 1986. Thermoelasticity. Pergamon, Oxford.
Nozaki, H., Taya, M., 1997. Elastic fields in a polygon-shaped inclusion with uniform eigenstrain. J. Appl. Mech. 64, 495–502.
Nozaki, H., Taya, M., 2001. Elastic fields in a polyhedral inclusion with uniform eigenstrains and related problems. J. Appl. Mech. 68, 441–452.
Okabe, M., 1979. Analytical expressions for gravity anomalies due to homogeneous polyhedral bodies and translations into magnetic anomalies. Geophysics 44, 730–741.
Okada, Y., 1985. Surface deformation due to shear and tensile faults in a half-space. Bull. Seism. Soc. Am. 75, 1135–1154.
Okada, Y., 1992. Internal deformation due to shear and tensile faults in a half-space. Bull. Seism. Soc. Am. 82, 1018–1040.
Ovid'ko, I.A., Sheinerman, A.G., 2005. Elastic fields of inclusions in nanocomposite solids. Rev. Adv. Mater. Sci. 9, 17–33.
Ovid'ko, I.A., Sheinerman, A.G., 2006. Misfit dislocations in nanocomposites with quantum dots, nanowires and their ensembles. Adv. Phys. 55, 627–689.
Pan, Y.C., Chou, T.W., 1979a. Green's function solution for semi-infinite transversely isotropic materials. Int. J. Eng. Sci. 17, 545–551.
Pan, Y.C., Chou, T.W., 1979b. Green's functions for two-phase transversely isotropic materials. J. Appl. Mech. 46, 551–556.

Pan, E., Yang, B., 2001. Elastostatic fields in an anisotropic substrate due to a buried quantum dot. J. Appl. Phys. 90, 6190–6196.
Pan, E., Yang, B., 2003. Elastic and piezoelectric fields in substrate AlN due to a buried quantum dot. J. Appl. Phys. 93, 2435–2439.
Pan, E., Albrecht, J.D., Zhang, Y., 2007. Elastic and piezoelectric fields in quantum wire semiconductor structures – A boundary integral equation analysis. Physica Stat. Sol. 244, 1925–1939.
Pan, E., 2002a. Elastic and piezoelectric fields around a quantum dot: fully coupled or semicoupled model? J. Appl. Phys. 91, 3785–3796.
Pan, E., 2002b. Elastic and piezoelectric fields in substrates GaAs (001) and GaAs (111) due to a buried quantum dot, J. Appl. Phys. 91, 6379–6387.
Pan, E., 2002c. Mindlin's problem for an anisotropic piezoelectric half-space with general boundary conditions. Proc. R. Soc. London A 458, 181–208.
Pan, E., 2004a. Eshelby problem of polygonal inclusions in anisotropic piezoelectric bimaterials. Proc. R. Soc. London A 460, 537–560.
Pan, E., 2004b. Eshelby problem of polygonal inclusions in anisotropic piezoelectric full- and half-planes. J. Mech. Phys. Solids 52, 567–589.
Paul, M.K., 1974. The gravity effect of a homogeneous polyhedron for three-dimensional interpretation. Pure Appl. Geophys. 112, 553–561.
Pearson, G.S., Faux, D.A., 2000. Analytical solutions for strain in pyramidal quantum dots. J. Appl. Phys. 88, 730–736.
Pohánka, V., 1988. Optimum expression for computation of the gravity field of a homogeneous polyhedral body. Geophys. Prosp. 36, 733–751.
Pohánka, V., 1998. Optimum expression for computation of the gravity field of a polyhedral body with linearly varying density. Geophys. Prosp. 66, 391–404.
Pryor, C., Pistol, M.E., Samuelson, L., 1997. Electronic structure of strained InP/$Ga_{0.51}$ $In_{0.49}$P quantum dots. Phys. Rev. B 56, 10404–10411.
Pryor, C., Kim, J., Wang, L.W., Williamson, A.J., Zunger, A., 1998. Comparison of two methods for describing the strain profiles in quantum dots. J. Appl. Phys. 83, 2548–2554.
Rinaldi, R., Cingolani, R., Lepore, M., Ferrara, M., Catalano, I.M., Rossi, F., Rota, L., Molinari, E., Lugli, P., Marti, U., Martin, D., Morier-Gemoud, F., Ruterana, P., Reinhart, F.K., 1994. Exciton Binding Energy in GaAs V-Shaped Quantum Wires. Phys. Rev. Lett. 73, 2899–2902.
Rodin, G.J., 1996. Eshelby's inclusion problem for polygons and polyhedra. J. Mech. Phys. Solids 44, 1977–1995.
Romanov, A.E., Beltz, G.E., Fischer, W.T., Petroff, P.M., Speck, J.S., 2001. Elastic fields of quantum dot in subsurface layer. J. Appl. Phys. 89, 4523–4531.
Romanov, A.E., Waltereit, P., Speck, J.S., 2005. Buried stressors in nitride semiconductors: influence on electronic properties. J. Appl. Phys. 97, 0437081–04370813.
Rongved, L., Frazier, J.T., 1958. Displacement discontinuity in the elastic half-space. J. Appl. Mech. 25, 125–128.
Rongved, L., 1955. Force Interior to One of Two Joined Semi-Infinite Solids. In: Bogdanoff, J.L. (Ed.), . In: in 2nd Midwestern Conf. Solid Mech, Vol. 129. Purdue University, Indiana, Res. Ser, pp. 1–13.
Ru, C.Q., Schiavone, P., Mioduchowski, A., 2001. Elastic fields in two joined half-planes with an inclusion of arbitrary shape. ZAMP 52, 18–32.
Ru, C.Q., 1999. Analytic solution for Eshelby's problem of an inclusion of arbitrary shape in a plane or half-plane. J. Appl. Mech. 66, 315–322.
Ru, C.Q., 2000. Eshelby's problem for two-dimensional piezoelectric inclusions of arbitrary shape. Proc. R. Soc. Lond. A 456, 1051–1068.
Ru, C.Q., 2001. A two-dimensional Eshelby problem for two bounded piezoelectric half-planes. Proc. R. Soc. Lond. A 457, 865–883.
Ru, C.Q., 2003. Eshelby inclusion of arbitrary shape in an anisotropic plane or half-plane. Acta Mechanica 160, 219–234.
Sen, B., 1951. Note on stresses produced by nuclei of thermo-elastic strain in a semi-infinite elastic solid. Quatr. Appl. Math. 8, 365–369.
Seo, K., Mura, T., 1979. The elastic field in a half space due to ellipsoidal inclusions with uniform dilatational eigenstrain. J. Appl. Mech. 46, 568–572.
Sharma, P., Dasgupta, A., 2002. Average elastic fields and scale-dependent overall properties of heterogeneous micropolar materials containing spherical and cylindrical inhomogeneities. Phys. Rev. B 66, 2241101–22411010.
Sharma, P., Ganti, S., 2004. Size-dependent Eshelby's tensor for embedded nano-inclusions incorporating surface/interface energies. J. Appl. Mech. 71, 663–671.
Shchukin, V.A., Bimberg, D., Malyshkin, V.G., Ledentsov, N.N., 1998. Vertical correlations and anti correlations in multisheet arrays of two dimensional islands. Phys. Rev. B 57, 12262–12274.
Singh, S.J., Kumari, G., Singh, K., 1999. Displacements and stresses due to a single force in a half-space in welded contact with another half-space. Geophys. J. Int. 139, 591–596.
Stangl, J., Holý, V., 2004. Structural properties of self-organized semiconductor nanostructures. Rev. Mod. Phys. 76, 725–785.
Steketee, J.A., 1958. On Volterra's dislocations in a semi-infinite elastic medium. Can. J. Phys. 36, 192–205.
Stoleru, V.-G., Pal, D., Touwe, E., 2002. Self-assembled (In,Ga)As/GaAs quantum-dot nanostructures: strain distribution and electronic structure. Physica E 15, 131–152.
Strakhov, V.N., Lapina, M.I., 1990. Direct gravimetric and magnetometric problems for homogeneous polyhedrons. Geophys. J. (UK) 8, 740–756.
Strakhov, V.N., Lapina, M.I., Yefimov, A.B., 1986. A solution of forward problems in gravimetry and magnetism with new analytical expressions for the field elements of standard approximating bodies. Izvestiya AN SSSR, Phys. Solid Earth 22, 471–482.
Stratton, J.A., 1941. Electromagnetic theory. McGraw-Hill, New York.

Takeuchi, H., Saito, M., 1972. Seismic surface waves. In: Bolt, B.A. (Ed.), . In: Methods of Computational Physics, Vol. 11. Academic Press, New York.

Thomas, A.L., 1993. Poly3D: a three dimensional, polygonal element, displacement discontinuity boundary element computer program with applications to fractures, faults, and cavities in the Earth's crust, Master's thesis, Stanford University.

Thomson, W., 1882. Note on the integration of the equations of equilibrium of an elastic solid. Lord Kelvin, Math. Phys. papers 1, 97–98.

Tian, L., Rajapakse, R.K.N.D., 2007. Analytical solution for size-dependent elastic field of a nanoscale circular inhomogeneity. J. Appl. Mech. 74, 568–574.

Tinti, S., Armigliato, A., 1998. Single-force point-source static fields: an exact solution for two clastic half-spaces. Geophys. J. Int. 135, 607–626.

Ursin, B., 1983. Review of elastic and electromagnetic wave propagation in horizontally layered media. Geophysics 48, 1063–1081.

Waldvogel, J., 1979. The Newtonian potential of homogeneous polyhedra. ZAMP 30, 388–398.

Walker, K.P., 1993. Fourier integral representations of the Green function for an anisotropic elastic half-space. Proc. R. Soc. Lond. A 457, 865–883.

Wang, L.W., Li, J., 2004. First-principle thousand-atom quantum dot calculations. Phys. Rev. B 69, 153302–153305.

Wang, C.D., Liao, J.J., 1999. Elastic solutions for a transversely isotropic half-space subjected to buried asymmetric load. Int. J. Numer. Anal. Meth. Geomech. 23, 115–139.

Wang, C.D., Tzeng, C.S., Pan, E., Liao, J.J., 2003. Displacements and stresses due to a vertical point load in an inhomogeneous transversely isotropic medium. Rock. Mech. Mining Sci. 40, 667–685.

Wang, Y.-C., Denda, M., Pan, E., 2006. Analysis of quantum-dot-induced strain and electric fields in piezoelectric semiconductors of general anisotropy. Int. J. Solids Struct. 43, 7593–7608.

Williams, D.P., Andreev, A.D., Faux, D.A., O'Reilly, E.P., 2004. Surface integral determination of build-in electric fields and analysis of exciton building energies in nitride-based quantum dots. Physica E 21, 358–362.

Williams, D.P., Andreev, A.D., Faux, D.A., O'Reilly, E.P., 2005. Derivation of build-in potentials in nitride-based semiconductor quantum dots. Phys. Rev. B 72, 2353181–23531810.

Woodhouse, J.H., 1974. Surface waves in a laterally varying layered structure. Geophys. J. Roy. Astr. Soc. 37, 461–490.

Wu, L., Du, S.Y., 1995a. The elastic field caused by a circular cylindrical inclusion. Part I: Inside the region $x_1^2 + x_2^2 < a^2$, $-\infty < x_3 < \infty$ where the circular inclusion is expressed by $x_1^2 + x_2^2 > a^2$, $-h \geqslant x_3 \geqslant h$. J. Appl. Mech. 62, 579–584.

Wu, L., Du, S.Y., 1995b. The elastic field caused by a circular cylindrical inclusion. Part II: Inside the region $x_1^2 + x_2^2 > a^2$, $-\infty < x_3 < \infty$ where the circular inclusion is expressed by $x_1^2 + x_2^2 > a^2$, $-h \leqslant x_3 \leqslant h$. J. Appl. Mech. 62, 585–589.

Wu, L., Du, S.Y., 1996. The elastic field in a half-space with a circular cylindrical inclusion. J. Appl. Mech. 63, 925–932.

Yang, B., Pan, E., 2002. Elastic analysis of an inhomogeneous quantum dot in multilayered semiconductors using a boundary element method. J. Appl. Phys. 92, 3084–3088.

Yang, B., Pan, E., 2003. Elastic fields of quantum dots in multilayered semiconductors: a novel Green's function approach. J. Appl. Mech. 70, 161–168.

Yu, H.Y., Rath, B.B., 2000. Micromechanics of defects in transversely isotropic solids with interfaces. Int. Mater. Rev 45, 241–269.

Yu, H.Y., Sanday, S.C., 1991. Elastic fields in joined half-spaces due to nuclei of strain. Proc. R. Soc. London A 434, 503–519.

Yu, H.Y., Sanday, S.C., Rath, B.B., 1992. Thermoelastic stresses in bimaterials. Phil. Mag., A 65, 1049–1064.

Yu, H.Y., Sanday, S.C., Chang, C.I., 1994. Elastic inclusion and inhomogeneities in transversely isotropic solids. Proc. R. Soc. London A 444, 239–252.

Yu, H.Y., Sanday, S.C., Rath, B.B., Chang, C.I., 1995. Elastic fields due to defects in transversely isotropic bi-materials. Proc. R. Soc. London A 449, 1–30.

Yue, Z.Q., 1995. Elastic fields in two joined transversely isotropic solids due to concentrated force. Int. J. Eng. Sci. 33, 351–369.

Zhang, X., Sharma, P., 2005. Size dependency in arbitrary shaped anisotropic embedded quantum dots due to nonlocal dispersive effects. Phys. Rev. B 72, 1953451–19534516.